Quaternary

Neogene

Paleogene

Cretaceous

Jurassic

Triassic

Permian

Carboniferous

Devonian

Silurian

Ordovician

Cambrian

Proterozoic

Volume 4

Chapter 16

Mapping Land Subsidence in Bogotá, Colombia, Using the Interferometric Synthetic Aperture Radar (InSAR) Technique with TerraSAR–X Images

Héctor MORA–PÁEZ[1]* (ID), Fredy DÍAZ–MILA[2] (ID), and Leonardo CARDONA[3] (ID)

1 hmora@sgc.gov.co
   Servicio Geológico Colombiano
   Dirección de Geoamenazas
   Grupo de Trabajo Investigaciones Geodésicas
   Espaciales (GeoRED)
   Diagonal 53 n.° 34–53
   Bogotá, Colombia

2 fdiaz@sgc.gov.co
   Servicio Geológico Colombiano
   Dirección de Geoamenazas
   Grupo de Trabajo Investigaciones Geodésicas
   Espaciales (GeoRED)
   Diagonal 53 n.° 34–53
   Bogotá, Colombia

3 leo.cardona.p@gmail.com
   Consultant
   Bogotá, Colombia

* Corresponding author

Abstract Bogotá, the capital city of Colombia, is the largest and most populous urban center in the country. Established in a moderate seismic zone, its complex topography facilitates the occurrence of landslides and floods. The city has been subject to a massive migration process in recent years, which has generated the accelerated urbanization of the city and increased its vulnerability to various natural hazards. Bogotá is located within the Sabana de Bogotá, a tectonic–sedimentary basin consolidated after the uplifting of the northern Andes approximately 5 Ma. With TerraSAR–X radar images, a quantitative analysis of the subsidence in the Sabana de Bogotá was carried out using the interferometric synthetic aperture radar technique for the city of Bogotá. The obtained results allowed establishing subsidence values in the central region of the city on the order of 3.3 cm/y. It is important to note that the BOGT GPS Continuously Operating Reference Station, which is part of a global network, indicates a decreasing value in its vertical component on the order of 3.5 ± 0.09 cm/y.

Keywords: subsidence, Sabana de Bogotá, interferometric synthetic aperture radar.

Resumen Bogotá, la capital de Colombia, es el centro urbano más poblado y grande del país. Establecida en una zona sísmica moderada, su compleja topografía facilita la ocurrencia de deslizamientos e inundaciones. La ciudad ha sido objeto de un proceso de migración masiva en los últimos años, lo cual ha generado la urbanización acelerada de la ciudad y un incremento en la vulnerabilidad ante diversas amenazas naturales. Bogotá está localizada en la Sabana de Bogotá, una cuenca tectonosedimentaria consolidada después del levantamiento del norte de los Andes hace aproximadamente 5 Ma. Mediante el uso de imágenes de radar TerraSAR–X se realizó el análisis cuantitativo de la subsidencia en la Sabana de Bogotá empleando la técnica de interferometría de radar de apertura sintética para la ciudad de Bogotá. Los resultados obtenidos permitieron establecer valores de subsidencia en la región central de la ciudad del orden de 3,3 cm/año. Es importante señalar que la estación GPS permanente de referencia denominada BOGT, que forma parte de la red global, indica un valor de descenso en su componente vertical del orden de 3,5 ± 0,09 cm/año.

Palabras clave: subsidencia, Sabana de Bogotá, interferometría de radar de apertura sintética.

1. Introduction

The generic term subsidence refers to the phenomenon that involves the settlement of the Earth's surface in a certain area due to several factors, which may be natural or anthropogenic caused by the impacts of various human activities (Poland, 1984; Poland et al., 1972,). Corapcioglu (1984) describes the phenomena of land subsidence, its main features and its occurrence in different parts of the world.

Natural subsidence is the result of the isostatic loading of sediments and natural compaction of Holocene deposits, or it could be the result of tectonic or volcanic processes. Subsidence of anthropogenic origin is the result of processes such as the heavy withdrawal of ground water, geothermal fluids, oil, and gas; the extraction of coal, sulfur, gold, and other solids through mining; underground construction (tunneling); or other mixed causes, such as the hydrocompaction of loosely deposited sediments, oxidation and shrinkage of organic deposits, the development of sinkholes in karstic terrain, and changes in the drainage of surface water and sediment load (Raucoules et al., 2007; UNESCO, 2018; Yuill et al., 2009). In some cases, it can affect buildings and urban infrastructure. This type of subsidence is generally of greater magnitude than natural subsidence (Meckel, 2008) and is the consequence of land modifications in environments with compressible deposits. Subsidence due to the removal of fluids, such as extractions of groundwater, oil, and gas, can reach values on the order of centimeters per year.

The phenomenon of subsidence has been observed in various places in the world, such as México, the United States, Thailand, Italy, France, Portugal, China, Taiwan, Vietnam, and Egypt. In North America, it is notable that the intense exploitation of aquifers that underlie various urban areas in México have generated high rates of subsidence. In the eastern sector of Mexico City, rapid subsidence is experienced due to the extraction of groundwater that exceeds the natural recharge and therefore compacts lacustrine sediments (Osmanoglu et al., 2011). Studies carried out by different authors using radar interferometry techniques show subsidence rates that reach up to 37 cm/y and indicate the spatial variation of the subsidence, which is closely related to the boundaries of the ancient lake of Texcoco and the thickness of its sediments (Cabral–Cano et al., 2008; Strozzi & Wegmuller 1999). In other cities in central México, the subsidence process occurs at relatively lower rates, between 4 and 9 mm per year, which remain high enough to cause significant surface faulting. These high subsidence rates are attributed to the increase in water demand due to population growth, which leads to a drop in groundwater level and the consolidation of sediments. The growth of the Mexican economy, especially in the most industrialized zone of central and northern México, suggests that the demand for water will continue to grow, which will increase the process of subsidence and the associated risks in various urban areas of the country (Chaussard et al., 2014; Universidad Nacional Autónoma de México, 2017).

There are several methods for monitoring land subsidence, including conventional practices and proven instrumental in–ground sensing systems (Tomás et al., 2009). The conventional techniques include repeated optical levelling and Global Positioning System (GPS) surveys, ground reconnaissance, photogeological analysis, groundwater monitoring, and the use of tape–extensometers. Advanced techniques include the processing and interpretation of interferometric synthetic aperture radar (InSAR), borehole tiltmeter and microseismic array data, excavations of monitoring trenches, and time domain reflectometry (TDR; Fergason et al., 2015). Traditionally, subsidence measurements have been based on obtaining GPS data or optical–leveling lines. Although these data provide accurate measurements, they require many hours of field work as well as the acquisition of data at specific sites and positions, which are spatially discrete although continuous over time and obtained at high sampling rates, 1 Hz, for example. GPS technology has some favorable characteristics. First, it depends very little on the nature of the surface in which the geodetic antenna is installed, although it requires the stability of such a surface as well as optimum visibility for the reception of signals from the satellites in the selected sites. Second, it has the ability to perform measurements on the three rectangular components, although the vertical component is less accurate than the horizontal components. On the other hand, the fundamental advantage of interferometry lies in the extensive spatial coverage of the measurements, which allows a good understanding of the phenomena to be studied, especially for the cases of complex morphologies. Monitoring land subsidence is one of the most successful applications of InSAR (Massonet & Souyris, 2008). It has been applied to many metropolitan areas and has shown that land subsidence is a rather common phenomenon occurring in various cities around the globe, including Las Vegas (Amelung et al., 1999; Burbey, 2002; Hoffmann et al., 2001), Los Angeles (Bawden et al., 2001), Mexico City (Cabral–Cano et al., 2008; López–Quiroz et al., 2009; Osmanoglu et al., 2011), Paris (Fruneau & Sarti, 2000; Fruneau et al., 2005), Naples (Tesauro et al., 2000), Venice (Bock et al., 2012; Teatini et al., 2007), Lisbon (Heleno et al., 2011), Jakarta (Bayuaji et al., 2010; Chaussard et al., 2013), Shanghai (Damoah–Afari et al., 2007), and Cairo (Aly et al., 2009). Most urban subsidence occurs as the result of excessive water withdrawal from underlying aquifers (Burgmann et al., 2000). Other causes for subsidence are hydrocarbon extraction, subsurface excavation (Burgmann et al., 2000), sediment compaction, and peat oxidation (Muntendam–Bos et al., 2009). Urban subsidence can induce various hazards. In low elevation coastal areas, subsidence can amplify flooding due to hurricane–induced surges (New Orleans and Houston), extreme tide conditions (Venice) (Bozzano et al., 2015; Lanari et al., 20004), and rising sea

Mapping Land Subsidence in Bogotá, Colombia, Using the Interferometric Synthetic Aperture Radar (InSAR) Technique with TerraSAR–X Images

Quaternary

levels (Bangkok). The flooding of New Orleans by hurricane Katrina demonstrated that the long–term effects of urban subsidence can lead to catastrophic consequences because the accumulated subsidence reduced the elevation of the protecting levees below their designed protective heights (Dixon et al., 2006; Yuill et al., 2009).

2. Land Subsidence in the Sabana de Bogotá

The Sabana de Bogotá, as it is locally known (i.e., Bogotá Savanna, a term that does not correspond to the geographical definition), is an old, slightly dissected plain of lacustrine origin located at an altitude of 2600 masl (meters above sea level) in the central axis of the Colombian Eastern Cordillera (Figure 1; Carvajal & Navas, 2016). It represents a tectonic–sedimentary basin consolidated after the final upheaval of the northern Andes at approximately 5 Ma (van der Hammen et al, 1973; Wijninga, 1996a, 1996b). It was a high–altitude lake with an area of 157 000 ha in the center of the Eastern Cordillera of the Colombian Andes that gradually filled with sediments during the uppermost Pliocene, Pleistocene, and Holocene (Figure 2). These horizontal sediments of lacustrine, fluvial, and fluvial–glacial origin are mostly clays, with thin intercalated silt, sand, and gravel lenticular beds and numerous layers. They also contain many ash layers, which come from the volcanoes located on the Central Cordillera. The aggregate thickness of the Pliocene – Quaternary units is some 600 m in the center of the former lake, and they thin out toward the edges and in the tributary river valleys. The Holocene sediments are unconsolidated, whereas the Pleistocene beds are semiconsolidated (Lobo–Guerrero, 1992; Lobo–Guerrero & Gilboa, 1987). The main city, the capital city of the country, is located within the Sabana de Bogotá. By 2018, the population of Bogotá was estimated as 7 378 400 inhabitants (Departamento Administrativo Nacional de Estadísticas, 2020). The urban development of Bogotá has progressed from the south in a northerly direction along the flanks of the mountains. These areas of higher relief are composed of sedimentary rocks, which are highly fractured and covered by thick colluvia, alluvia, river terrace sands and gravels, as well as fluvio–glacial and fan deposits (Ojeda & Donnelly, 2006).

In Colombia, subsidence occurs in major cities and causes structural damage to buildings and infrastructure. The land subsidence in Colombia was classified as the fourth risk in building the Formal Housing Index (FHI; Arbeláez et al., 2011). Bogotá is the largest and most populous city and has a high concentration of natural hazards. Located in a moderate seismic zone, its complex topography makes it prone to landslides and floods; in addition to these geographical factors, mass migration and unbridled growing urbanization processes in recent years make it susceptible to the increase in vulnerability to geodynamic phenomena.

During the last 60 years, numerous tube–wells have been constructed in the Sabana de Bogotá to supply groundwater for irrigation, several town aqueducts and numerous factories. Lobo–Guerrero (1995) showed two case studies to prove the descent of the groundwater potentiometric level in the western portion of the artesian Sabana de Bogotá basin. The first case, located in Facatativá in the western part of the Sabana de Bogotá (Figure 3), documents the groundwater level descent in free aquifers of the Guadalupe Formation over 24 years. The second, in the El Rosal region (Figure 3), presents descent in artesian leaky aquifers in the Sabana and Tilatá Formations during 1990–1995. All groundwater users in the basin face a problem: They have to pump deeper every year and must replace wells for others of higher cost. This takes place precisely when surface water resources are insufficient to satisfy demand. Groundwater level descent is the main cause of uneven compaction and land subsidence observed in surface layers of the Sabana Formation, of severe damage to construction and pavement, and of overpressure in deep water wells. Therefore, it is possible to say that negative experiences in the México valley, also composed of nonconsolidated lacustrine sediments, are being repeated in the Sabana de Bogotá. Subsidence due to uncontrolled groundwater extraction is now well understood by hydrogeologists and may be remedied. Groundwater are indispensable for several towns, agricultural irrigation, and industrial applications in the Sabana de Bogotá. The regional lowering of the potentiometric level has caused the disappearance of mountain front springs, streams, and wetlands, as well as land subsidence, cracks on the ground, in buildings and roads, well collapses, the fall down of submersible pumps, and replacements with deeper wells (Lobo–Guerrero, 2003). Other authors and institutions have also carried out advanced research on subsidence in the Sabana de Bogotá. Among the studies aimed at illustrating this phenomenon, those prepared by the Departamento Administrativo del Medio Ambiente (DAMA; Departamento Administrativo del Medio Ambiente, 1999), Antonio–Fragala & Obregón–Neira (2011), the Universidad Nacional de Colombia (2011), and Veloza (2013) stand out, to name a few.

3. Methodology

Subsidence can be quantified by means of spatial geodesy techniques, both through Global Navigation Satellite System (GNSS) based methods of high precision positioning, and through imaging geodesy. Imaging geodesy uses radar images and the InSAR technique, that is, the measurement of signal phase change over different time periods (Sousa et al., 2013). The Earth's surface is illuminated with synthetic aperture radar (SAR), with short pulses radiated by a radar antenna (Deutsches Zentrum für Luft– und Raumfahrt [DLR], 2009). The radar pulse is reflected from the Earth's surface, and the so–called radar echo is again received by the antenna and recorded. Fig-

Figure 1. Location of the Sabana de Bogotá high plain (yellow area) with respect to Colombia and South America.

ure 4 corresponds to a representation of the fundamentals of InSAR. The satellite, when making its first pass over the terrestrial surface, establishes what is known as the initial ground surface, and obtains the radar waves that are reflected from the surface. Subsequently, depending on the time interval of taking images from the different space platforms that exist, the satellite makes a second pass and obtains the radar signals reflected from the surface. If there are changes in the surface of the ground between the data collection period of the two images (two passes) (subsided ground surface), it is possible
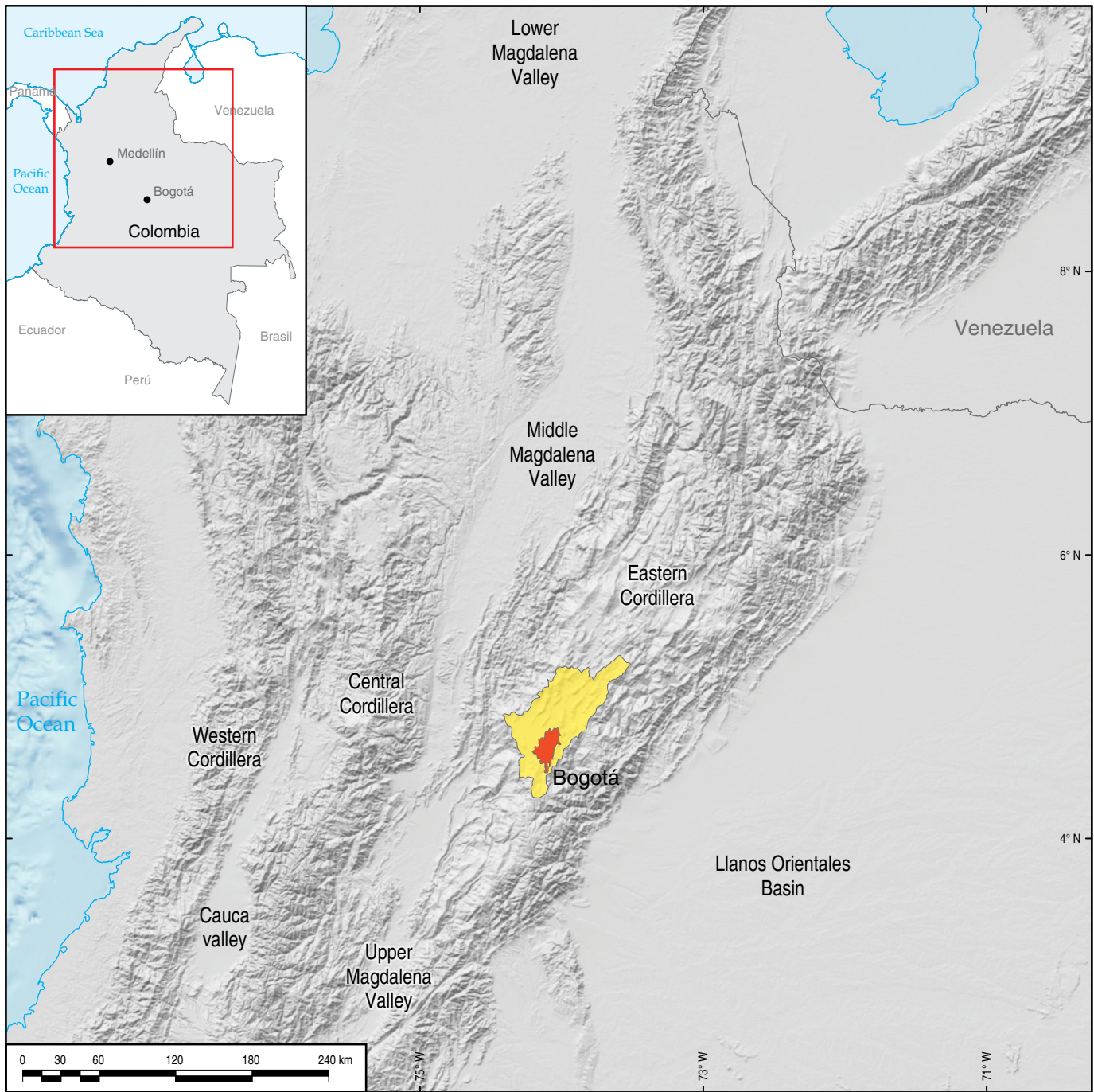
Mapping Land Subsidence in Bogotá, Colombia, Using the Interferometric Synthetic Aperture Radar (InSAR) Technique with TerraSAR–X Images

Quaternary

Figure 2. Location of the Sabana de Bogotá (yellow area) and Bogotá city (red area) on the Eastern Cordillera.

to observe a phase difference in the radar waves by comparing the signals obtained between the two satellite passes, as shown in Figure 4, waves A to E; in other words, away from the satellite in this case. This phase difference of the waves is used to estimate the component of ground movement along the line of sight of the satellite (either to or from the satellite), which is represented by a color as part of a complete cycle of color. Since this technique is based on the phase difference of multiple waves, the accuracy is limited by the detectable fractions

of the radar wavelength (λ) that is used (Bürgmann et al., 2000; Global Volcanism Program, 2012).

Without going into detail about the steps associated with generating interferograms, which are not the purpose of this article, some basic elements are presented. SAR systems record both the amplitude and phase of the backscattered echoes. The phase of each pixel of a focused SAR image is the sum of three distinct contributions: (a) The two–way travel path (sensor–target–sensor: Hundreds of kilometers in the satellite
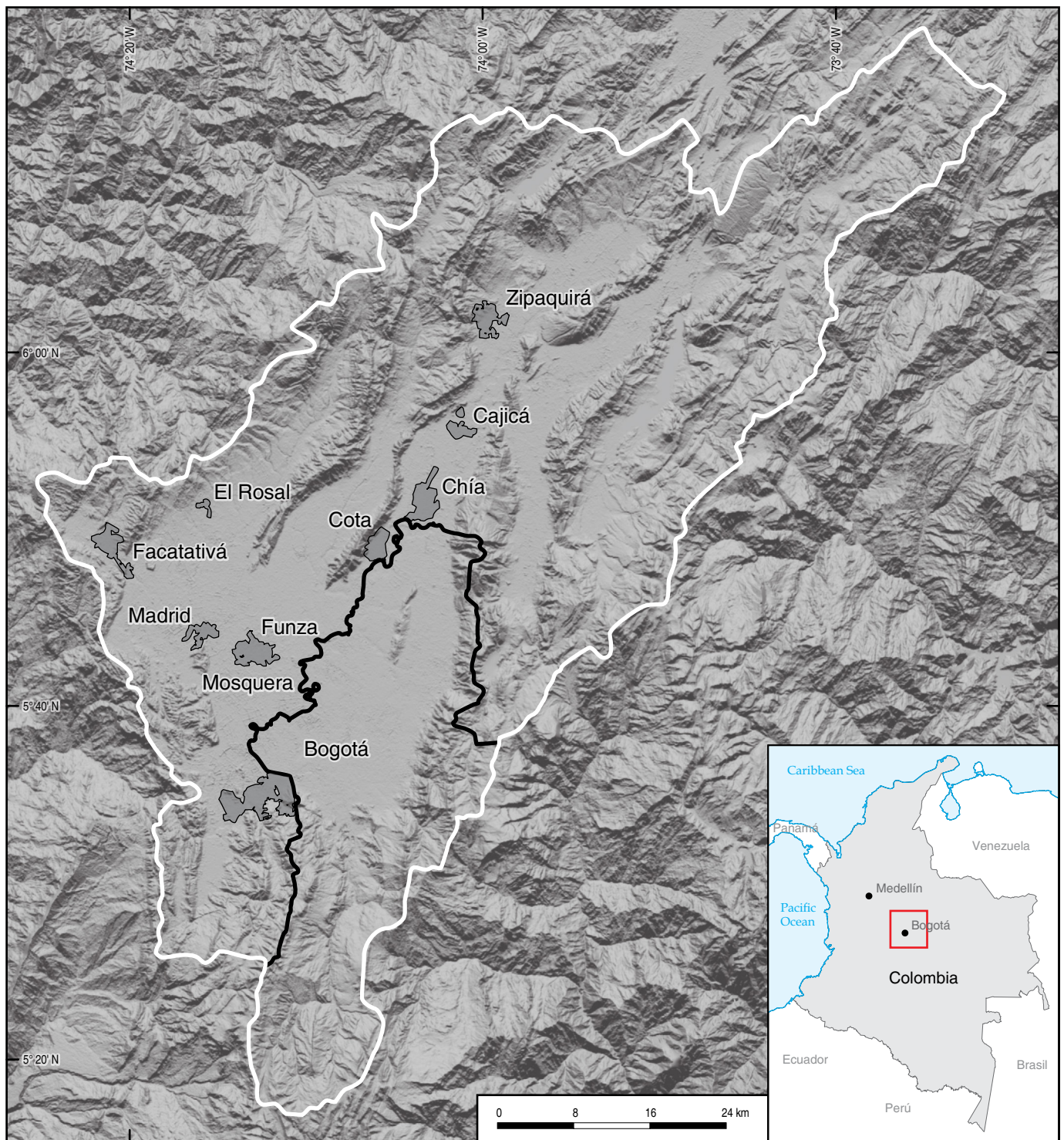
Figure 3. Boundary of the Sabana de Bogotá (white line), perimeter of Bogotá city (black line), and some towns (dark gray areas) located near to Bogotá city.

case) that, divided by the used wavelength (a few centimeters), corresponds to millions of cycles; (b) the interaction between the incident electromagnetic waves and the scatterers within the ground resolution cell; (c) the phase shift induced by the processing system used to focus the image. Therefore, the phase of a single SAR image is of no practical use. In contrast, if two SAR images from slightly different viewing angles are considered (an interferometric pair), their phase difference (interferometric fringes) can be usefully exploited to monitor terrain changes (Rocca et al., 2014).

An InSAR interferogram is an image formed by the difference of two coregistered SAR phase images (Zhou et al., 2009).
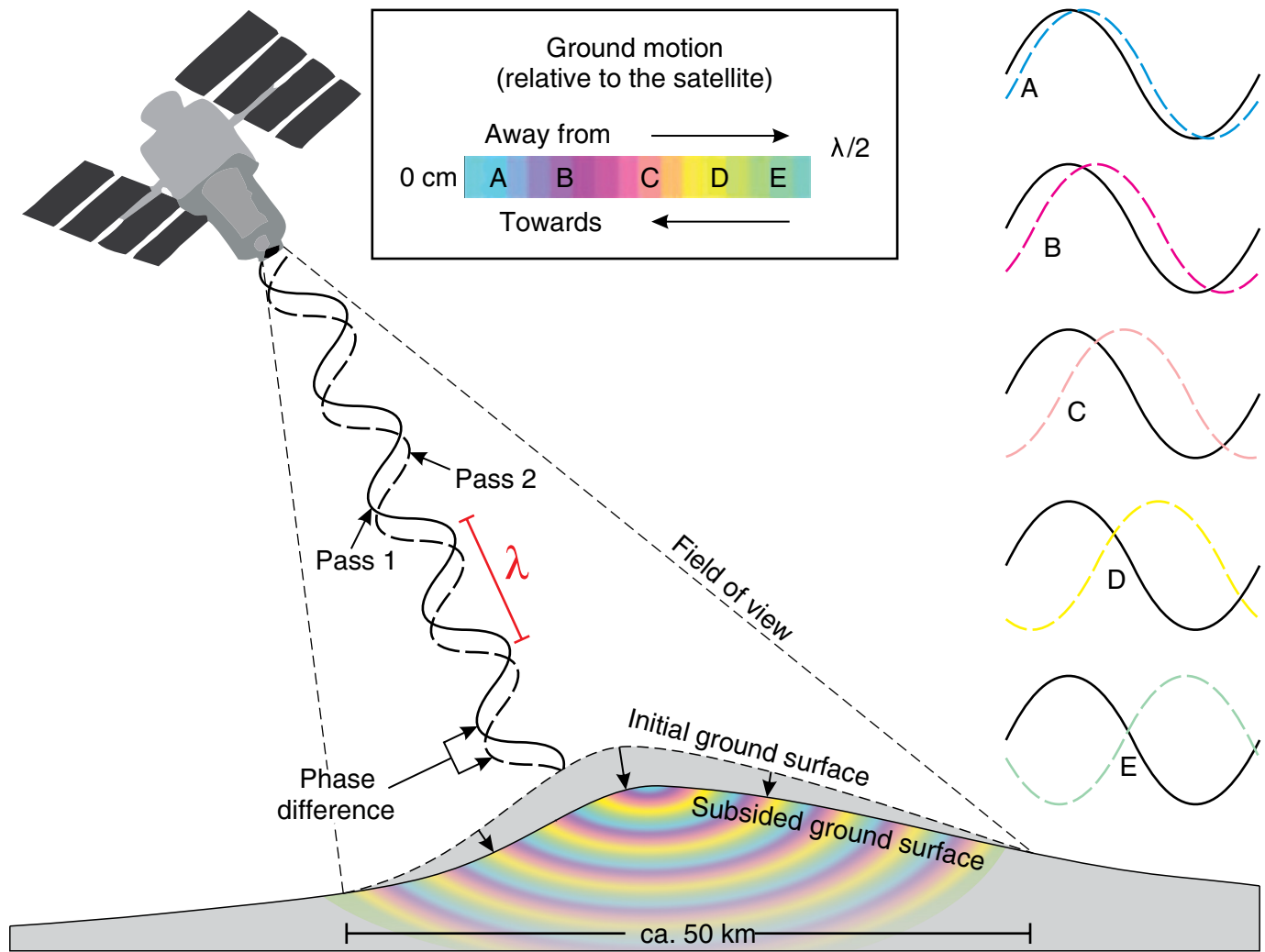
Mapping Land Subsidence in Bogotá, Colombia, Using the Interferometric Synthetic Aperture Radar (InSAR) Technique with TerraSAR–X Images

Quaternary

Figure 4. Representation of the fundamentals of InSAR application to subsidence studies. Modified from Global Volcanism Program (2012).

It represents a relative change in the earth's surface, especially vertical displacement of the ground. For its generation, two images are required to establish if there are terrain changes over the time interval defined by the date of acquisition of each image. The reference image acquired in the first pass is known as the "master", and the image taken in the second pass is called the "slave" (Figure 5). The SAR interferogram is generated by cross–multiplying, pixel by pixel, the first SAR image (master) with the second one (slave) (Ferreti et al., 2007). The interferogram is represented by fringes of complete color cycles (red, orange, yellow, green, blue, and purple) that allow determination of the relative displacement of one site compared to another, as shown in Figure 6 (U.S. Geological Survey, 2017). A fringe is a line of equal phase in the interferogram, and the number of fringes is counted from a reference point where the surface displacement is supposedly zero (Zhou et al., 2009). The colored fringes observed in an InSAR image can be regarded like contour lines on a map. The order of the colors indicates whether the image

corresponds to an uplift or sinking of the ground, i.e., subsidence. Each interferogram is, in turn, subjected to additional processing called phase unwrapping, that is, the process of recovering unambiguous phase data that are measured modulo 2π rad (wrapped data) (Goldstein et al., 1988; Hooper & Zebker, 2007). These unwrapped images are digitally stacked in a three–dimensional cube of data; the dimensions correspond to range direction, azimuth, and number of interferograms (Agram et al., 2012a), as shown in Figure 7. This processing permits generation of maps of accumulated displacements, velocities per year, and time series.

3.1. Previous Studies

3.1.1. GPS Positioning

The GPS IGS BOGT (Bogotá) station was installed on 4 November 1994, under a partnership between National Aeronautics and Space Administration (NASA) and the Servicio
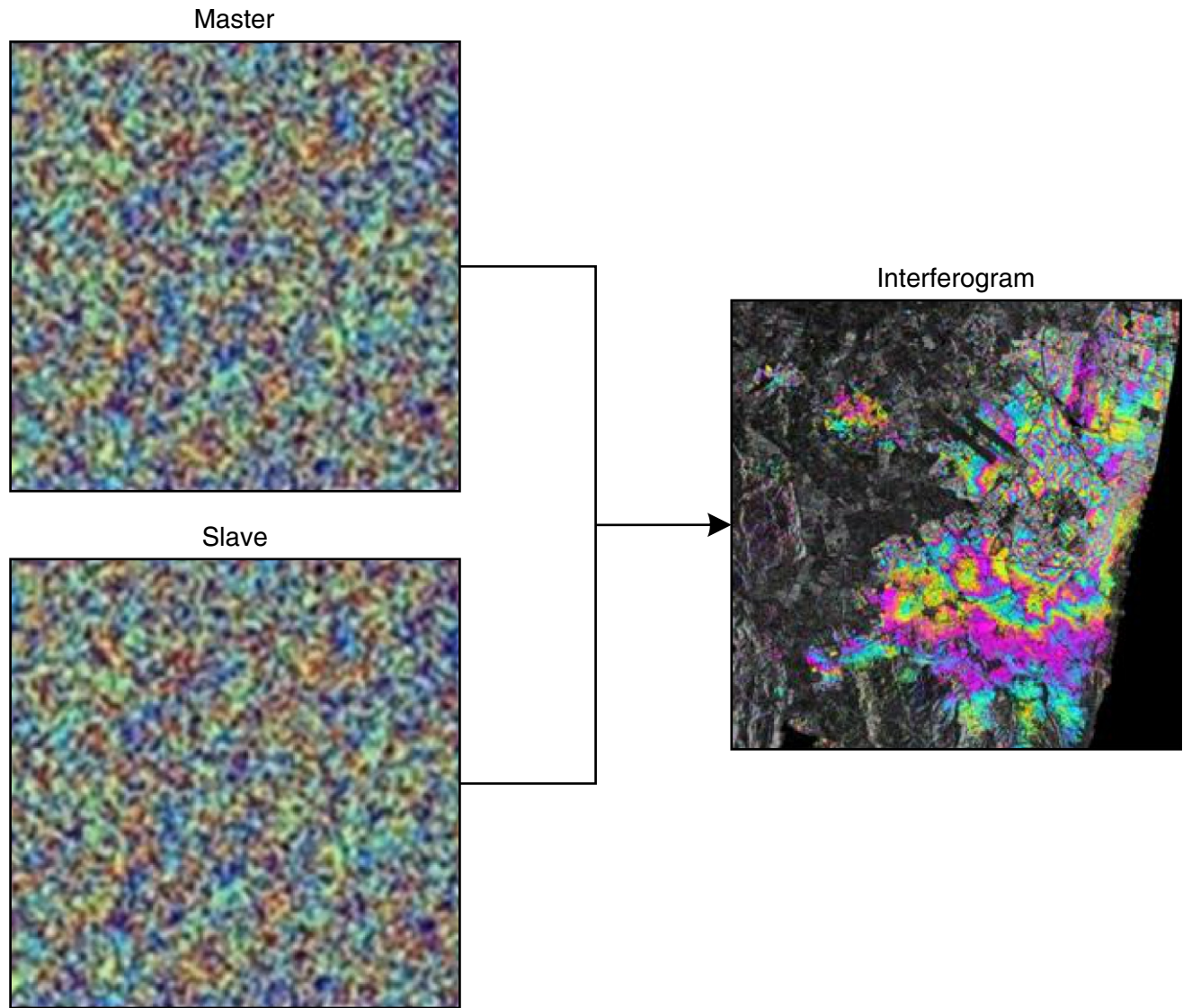
Master

Slave

Interferogram

Figure 5. Example of the generation of an interferogram of Bogotá city.

Geológico Colombiano (SGC). Kaniuth et al. (2001) analyzed data from the BOGT station together with another station, BOGA, that is located on the top of the Instituto Geográfico Agustín Codazzi (IGAC) 11–floor building. The two stations are separated by approximately 180 m. Previous episodic GPS measurements at the BOGA marker as well as spirit levelling between the BOGT and BOGA stations indicated that the IGAC building might be subsiding. Their analysis comprises the data processing between BOGA and a permanent station also located atop a building in Cartagena city, corresponding to a 656 km baseline, and obtained a vertical component of –25.2 ± 1.4 mm/y for the BOGA station. They considered that this vertical velocity seems to apply not only to the BOGA station located on the 11–floor building but also to the BOGT station that is set up on the ground. They also considered, from the GPS results, that the IGAC building, which was constructed between 1953 and 1955, is probably tilting. Rudenko et al.

(2013) reprocessed GPS data from 266 stations with a tracking history longer than 2.5 years and found that the BOGT station has a vertical trend of –44.21 ± 0.19 mm/y, which is almost twice the value obtained by Kaniuth et al. (2001). The Space Geodesy Research Group of the SGC runs the GeoRED project, which corresponds to the implementation of the GNSS Satellite Geodesy National Network for geodynamic purposes (Mora–Páez, 2006; Mora–Páez et al., 2013, 2018, 2020). Under the frame of this project, GPS data obtained from the BOGT station are processed using GIPSY–OASIS II software version 6.3 developed by the Jet Propulsion Laboratory (JPL) of the California Institute of Technology (Bertiger et al., 2010; Zumberge et al., 1997). The BOGT station velocity is computed using HECTOR software (Bos et al., 2013), a package developed at SEGAL (Space & Earth Geodetic Analysis Laboratory at the University of Beira Interior, Portugal) that is able to take into account temporal correlations in the data to

Mapping Land Subsidence in Bogotá, Colombia, Using the Interferometric Synthetic Aperture Radar (InSAR) Technique with TerraSAR–X Images

Quaternary

estimate the associated uncertainties. HECTOR is based on the maximum likelihood estimation (MLE), which is the method of prediction in the stochastic modeling of the GPS time series. Figure 8 corresponds to the BOGT time series of the vertical component, which allows the observation of continuous downward behavior that corresponds to a linear trend estimation of –3.45 ± 0.09 cm/y velocity, assuming a white noise model and generated using HECTOR software; a seasonal signal is included in the estimation process. The figure also shows the offsets associated with changes to the antenna, receiver, or both, and, in some cases, firmware updates, issues that are very important to take into account in order to obtain a very reliable estimation of the GPS time series.

3.1.2. Imaging Geodesy

Previous InSAR results in Bogotá were obtained by the Cartographic Institute of Catalunya (CIC) under a consulting contract for FOPAE (Fondo para la Prevención y Atención de Emergencias), which is the former Oficina de Prevención de Desastres in Bogotá city. Scenes from European Remote Sensing satellite (ERS–1, ERS–2) and Earth observation ENVIronmental SATellite (Envisat) were used from 1992 to 2005; in addition, Envisat scenes were used to obtain vertical maps from 2006 to 2009 (Instituto Cartográfico de Cataluña, 2007, 2009; Instituto Cartográfico y Geológico de Cataluña, 2014). Envisat was launched on 1 March 2002, (Wegmüller et al, 2009), and the European Space Agency declared the end of the mission on 9 May 2012. Figure 9 corresponds to a map of the linear velocity of deformation in the urban area of Bogotá city obtained using 19 Envisat images covering the time period between October 1997 and January 2009 (11.12 years), with a maximum value of 8 cm/y (Cartographic Institute of Catalunya, 2009).
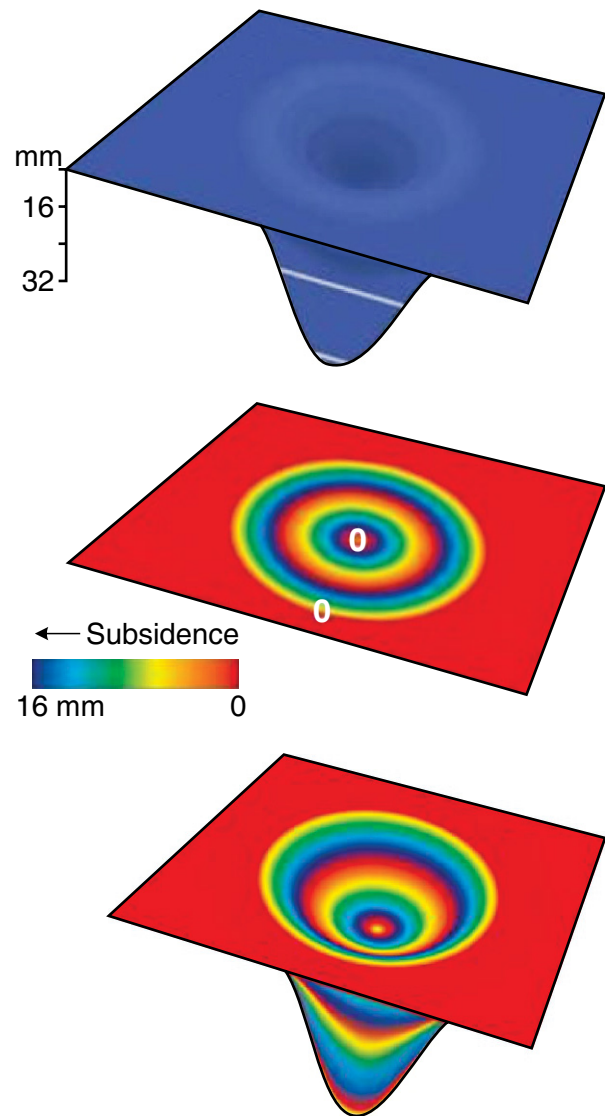
4. Results

TerraSAR–X is a German Earth–observation satellite that was launched in 2007. We used 76 SAR images from descending track acquired by the TerraSAR–X satellite from 28 September 2011 to 17 October 2017. The wavelength of those acquisitions is 31 mm, which corresponds to the X–band in the electromagnetic spectrum, and the spatial resolution is 3 m. The X–band is less suitable for vegetated areas due to the limited penetrating capability compared to L or even C–bands; however, it is approximately twice as sensitive to small deformation incidents (Le et al., 2016).

4.1. Interferograms

A set of interferograms was generated to estimate the vertical displacement in Bogotá associated with land subsidence. These images were processed using the ISCE (InSAR Scientific Com-

Figure 6. Illustrative example of the form of representation of a vertical displacement (subsidence) from one point compared to another. In this case, the strip of radar images corresponds to one cycle of colors representing 16 millimeters that is the half–wavelength of the TerraSAR–X image. Adapted and modified from U.S. Geological Survey (2017).

puting Environment) scientific software package (Agram et al., 2016; Gurrola et al., 2010; Rosen et al., 2009; 2012, 2015), which was designed from the ground up as a geophysics community tool for generating stacks of interferograms that lend themselves to various forms of time–series analysis, with attention paid to accuracy, extensibility, and modularity. Its initial development was funded by NASA's ESTO (Earth Science Technology Office) under the AIST (Advanced Information Systems Technology) in 2008 and is currently being funded under the NASA–ISRO SAR (NISAR) project. ISCE can process data from the Advanced Land Observing Satellite (ALOS–1, ALOS–2) from Japan, ERS, Envisat, the Constellation of Small Sat-
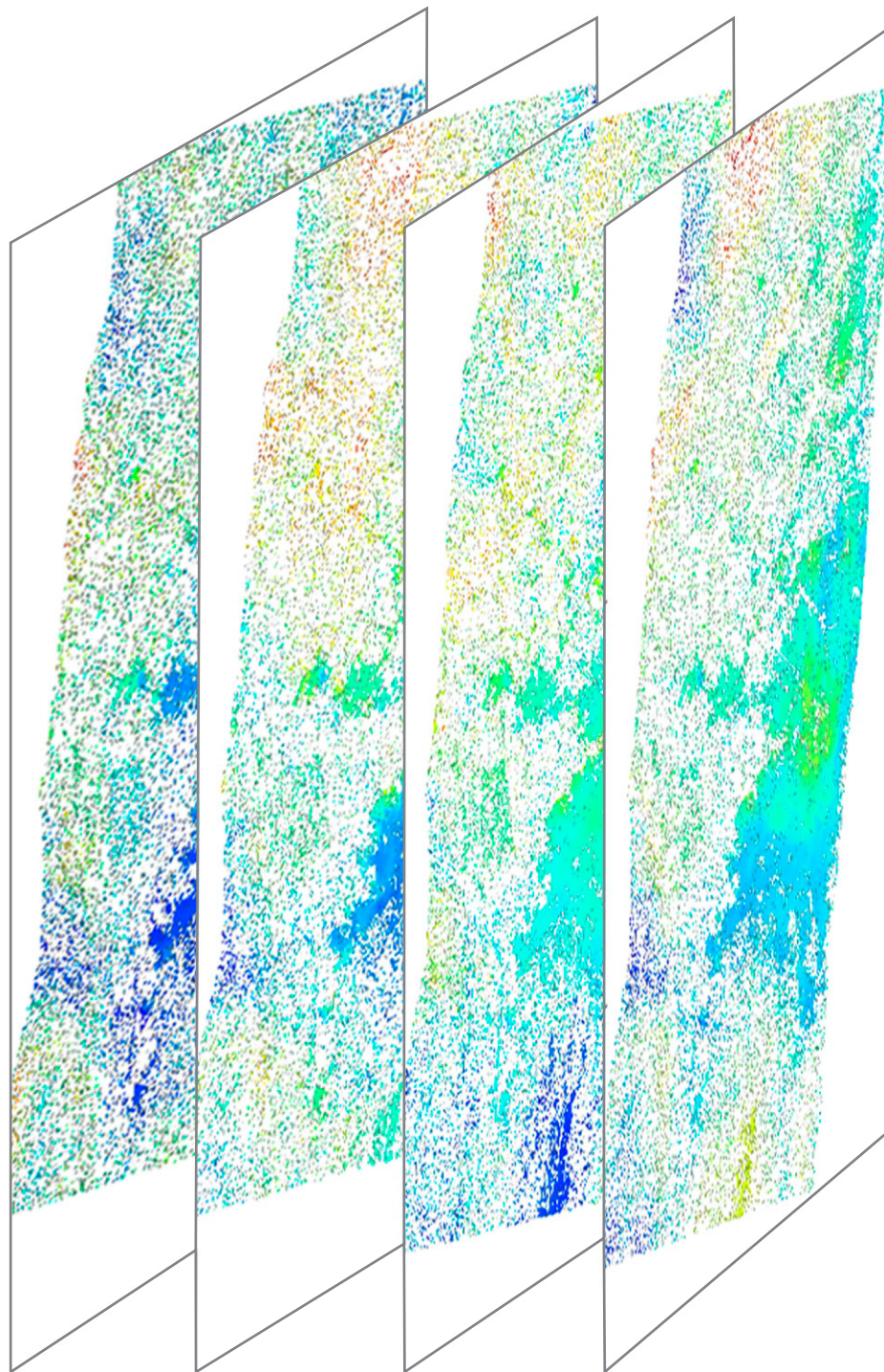
Figure 7. Example that represents how the unwrapped images are digitally stacked in a 3–D cube of data.

ellites for Mediterranean basin Observatory (Cosmo–SkyMed) from Italy, Canadá's Earth observation satellite (RADARSAT–1, RADARSAT–2), the European Space Agency satellites (Sentinel–1; Sentinel–2), and the German TerraSAR–X platforms. The InSAR technique measures ground displacement in the radar line–of–sight (LOS) by computing the phase difference of two SAR images that are temporally separated. The LOS is converted into a vertical displacement taking into consideration the satellite incidence angle. The incidence angles of the TerraSAR–X images used in this study are in the range of 31.5° and 34.76°; thus, an average value of 33.2° was adopted as the incidence angle for processing. To remove the topography, ISCE software undertakes a simulation of the radar image amplitude from a digital elevation model (DEM) and the reference track, projects
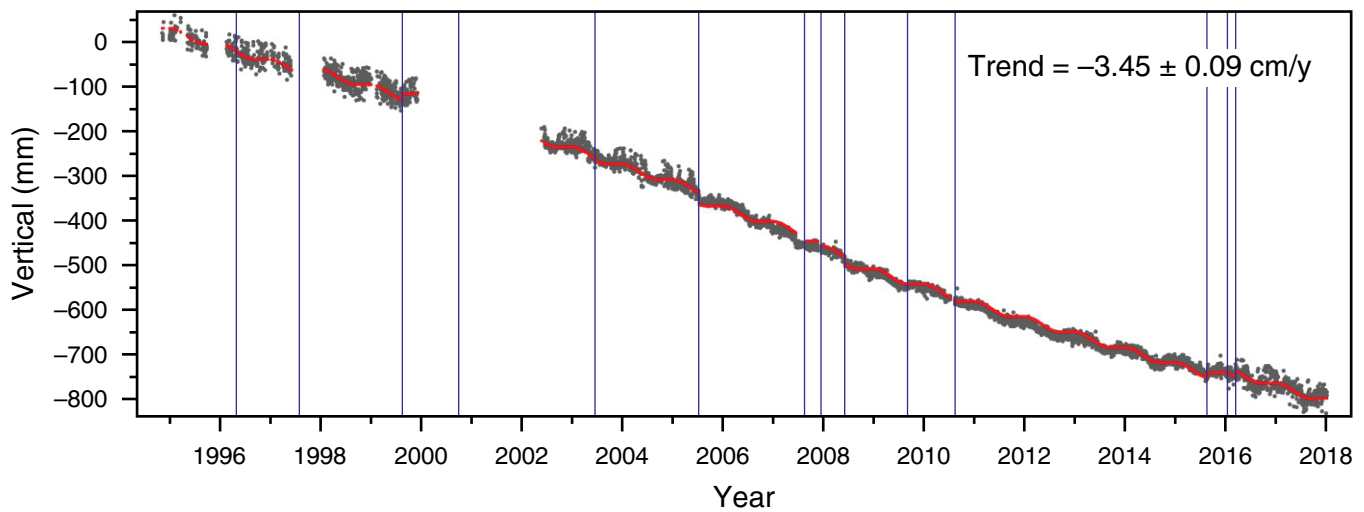
Mapping Land Subsidence in Bogotá, Colombia, Using the Interferometric Synthetic Aperture Radar (InSAR) Technique with TerraSAR–X Images

Quaternary

Figure 8. Vertical time series from the GPS IGS BOGT station. Gray dots are the daily positions obtained using GIPSY–OASIS II software; the red line is a polynomial trend that corresponds to the behavior of the GPS station. The velocity value is obtained as a linear trend. Blue lines indicate offsets associated with the change of geodetic instruments, such as the antenna or receiver.

the elevations into the radar coordinates of the interferogram, then calculates the topographic phase and subtracts it from the original interferogram. The NASA Shuttle Radar Topography Mission (SRTM) DEM version 3 was used to remove the topographic components from SAR interferograms.

When the interferogram has been corrected for the topographic phase, ISCE calculates the spatial correlation of the phase as a proxy for interferometric coherence (Rosen et al., 2012). There are two important issues that must be considered for InSAR processing: Coherence and baseline. The first implies that the phase can be estimated from the interferometric SAR pair by means of the local coherence, which is the cross–correlation coefficient of the SAR image pair estimated at a small window, once all the deterministic phase components are compensated for. In an interferogram, coherence is a measure of correlation; it ranges from 0 (there is no useful information in the interferogram, the interferometric phase is just noise), to 1 (there is no noise in the interferogram), in other words, it is a perfect interferogram, with a complete absence of phase noise. The coherence can be affected by several factors, such as local slope, properties of the surface being imaged, time lag between the passes in an interferogram, the baseline (because large baselines lead to low coherence), and technical details of the generation of the interferogram (European Space Agency, 2014). The second, the baseline, corresponds to the distance between the two satellites (or orbits) in the plane perpendicular to the orbit, and its projection perpendicular to the slant range is called the perpendicular baseline (Ferreti et al., 2007). The resulting stack of interferograms are inverted using the NSBAS (new small baseline subset) method proposed by Doin et al. (2011) that permits, in this case, building the temporal evolution of the displacement associated with the subsidence phenomena in Bogotá. The NSBAS package is a fully automatic chain of

processing that produces a timeline of the line of sight surface movement over an area. It has been especially optimized for monitoring transient ground motions of small amplitude taking place over large areas and in natural settings. NSBAS corresponds to an extension of the SBAS (small baseline subset) approach developed by Berardino et al. (2002) that permits using a regularization function to compensate for missing links in the interferometric networks that produce lack of temporal and geometrical overlaps, which generates temporal and spatial correlations (Agram et al., 2013; López–Quiroz et al., 2009).

For this study, 319 interferograms were generated, of which 258 were selected for this study; these are connected by a network (Figure 10). The selected interferograms have a baseline of less than 250 m, following the conclusions about the optimal parameters of determination and control of the TerraSAR–X satellite orbit according to the analyses carried out by Arbinger et al. (2004), Eineder et al. (2003), and Kahle & D'Amico (2014). Thus, the limit established in our baselines avoids low coherence interferograms in the processing that can affect the results. For example, the results of this processing can be observed in Figure 11a–l, in which twelve interferograms generated by the combination of thirteen images acquired on different dates are presented.

4.2. Ground Displacement Maps and Time Series

To quantify the displacements associated with the subsidence in Bogotá, GIAnT (Generic InSAR Analysis Toolbox) software has been used (Agram et al., 2012a, 2012b, 2013). GIAnT is a user–friendly, open–source, documented framework for the rapid generation of time series of surface displacements using InSAR data, and it is configured to work with several outputs of processing packages, such as ISCE.
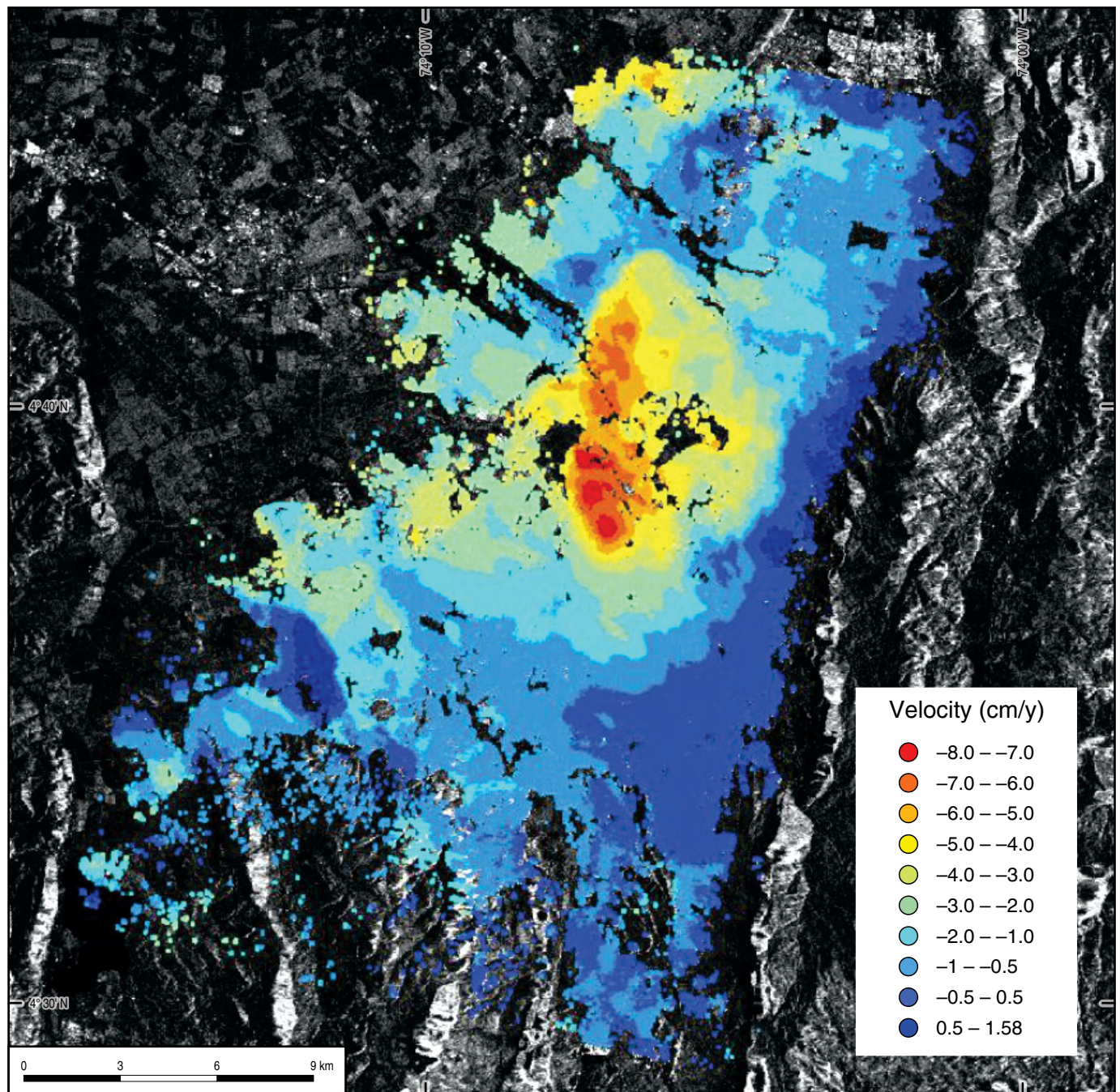
Figure 9. Map of linear velocity of deformation in the urban area of Bogotá city obtained from Envisat scenes, October 1997–January 2009. Modified from ICC (2009).

As a result of the processing of the TerraSAR–X images, a map of the subsidence model for Bogotá from 28 September 2011 to 17 October 2017 was obtained by combining interferometric pairs. The maximum observed velocity value corresponded to 3.3 cm/y, which was observed in the central sector of the city (Figure 12) and corresponds to a wide zone with scattered patches with similar tendencies and concentrated within the same area; however, there is one area that stands out above the others. Likewise, three time series are generated

for three selected sites; high, medium, and low values of subsidence are presented (Figure 13). Each time series is generated with GIAnT, Figure 14, which uses a Gaussian weighted moving average filter that allows a discrepancy between raw displacement observations (black circles) and filtered observations (red crosses) to be established (Figure 14). Site 1 is located within the area that has the highest subsidence (3.3 cm/y) (Figures 13, 14a), in the industrial area named Puente Aranda. Site 2, the medium value (2 cm/y) (Figures 13, 14b),
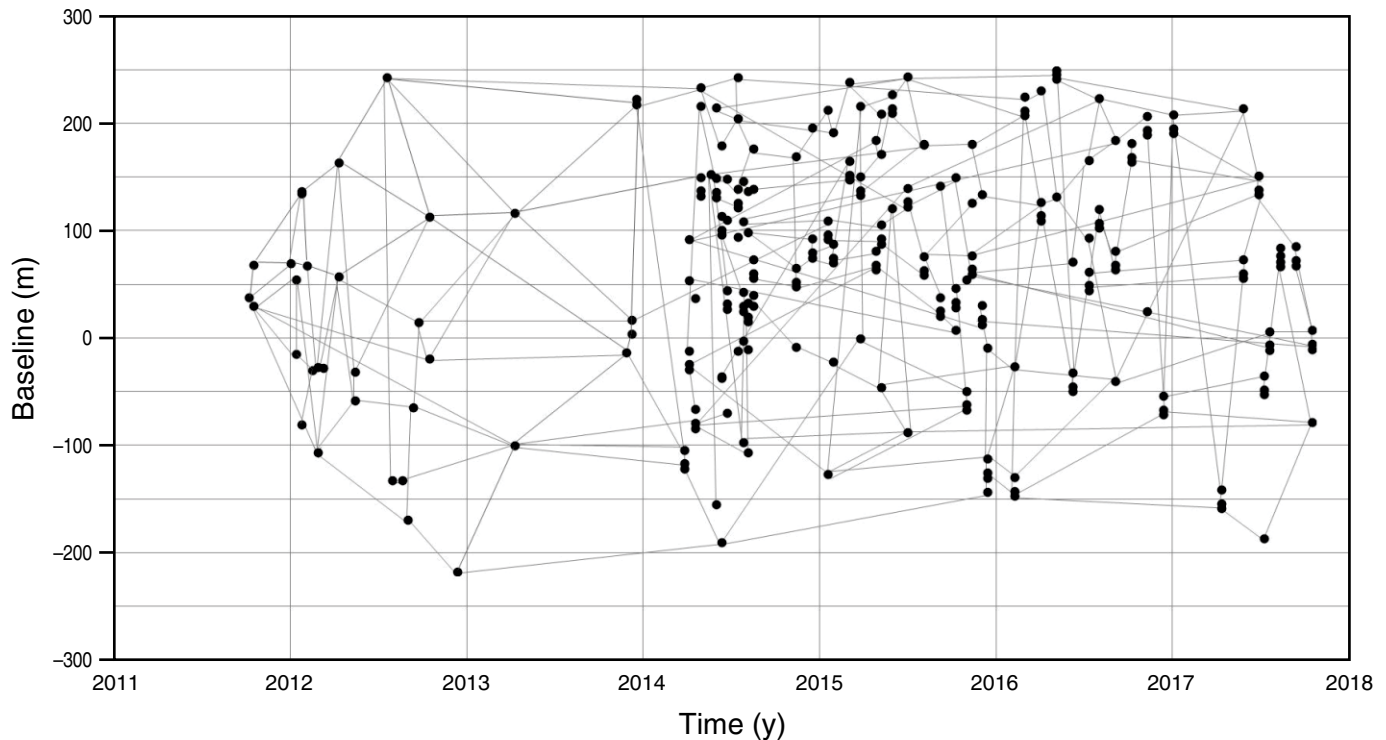
Mapping Land Subsidence in Bogotá, Colombia, Using the Interferometric Synthetic Aperture Radar (InSAR) Technique with TerraSAR–X Images

Quaternary

Figure 10. Network of selected interferograms for the generation of the vertical displacement map and time series map.

is in the Normandía site to the southeast from the El Dorado Airport in the city of Bogotá. Site 3, the low value (0 cm/y) (Figures 13, 14c), is in La Guaca sector.

For the correct assessment of any detected deformation and its time evolution, it is necessary to perform an error estimation of the interferometric techniques. GIAnT software enables mitigation of the effects of signal delays due to the stratified troposphere in each interferogram using either an empirical approach or estimates from global atmospheric models (Agram et al., 2013).

To estimate the uncertainty of the time series of this study, the statistical approach known as a jackknife is used. Thus, from an original set of interferograms, successive subsets of interferograms are generated excluding a SAR image each time; the terms corresponding to the linear velocity and seasonal are re–estimated for each of the subsets (Agram et al., 2013). The standard deviation of the estimated time series of the dataset represents the uncertainty for each epoch corresponding to the images. The master image is included in all subsets and is used as a reference. Time series are estimated only in those pixels that are coherent in all interferograms; a 0.2 value is used as a minimum coherence value to obtain a sufficient number of pixels in the selection. Table 1 shows the uncertainty values for the three selected sites, to which the time series of Figure 14a, 14b, 14c correspond. These sites are those with the highest, medium, and low velocity values, respectively.

5. Conclusions and Recommendations

An analysis of the SAR images used in this study in Bogotá shows a distributed subsidence pattern in the urban area with maximum values in the central part of the city. However, in the short–term, it is necessary to establish if the observed subsidence originates mainly from the groundwater withdrawal from the local aquifer, or it is a natural result due to compaction of the zone, or both possibilities. The TerraSAR–X results present very good distribution and spatial resolution for use in addressing the subsidence inside the city of Bogotá.
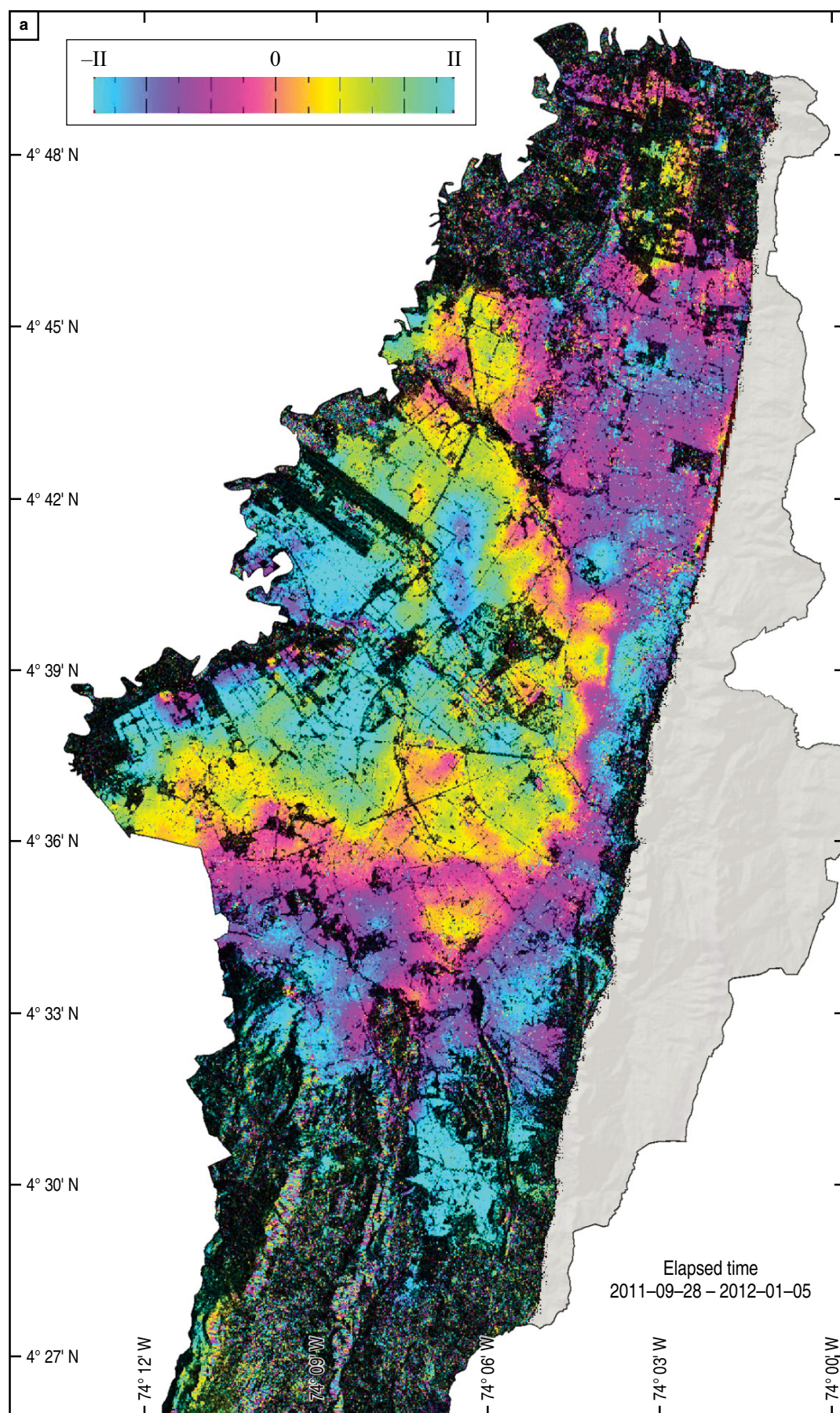
It is important to consider that the soil of the city of Bogotá is constituted geologically by clay deposits formed by the drying of an ancient lake, with intermediate and discontinuous layers of sand and organic soils. The thickness of the deposits increases gradually from the areas near the eastern hills, with a few meters of depth, to the western sector, with sediments up to 600 m thick. In the middle part of the city, close to the Universidad Nacional de Colombia and the SGC, the thickness varies between 180 and 200 m. These are large layers of relatively soft and compressible soils.
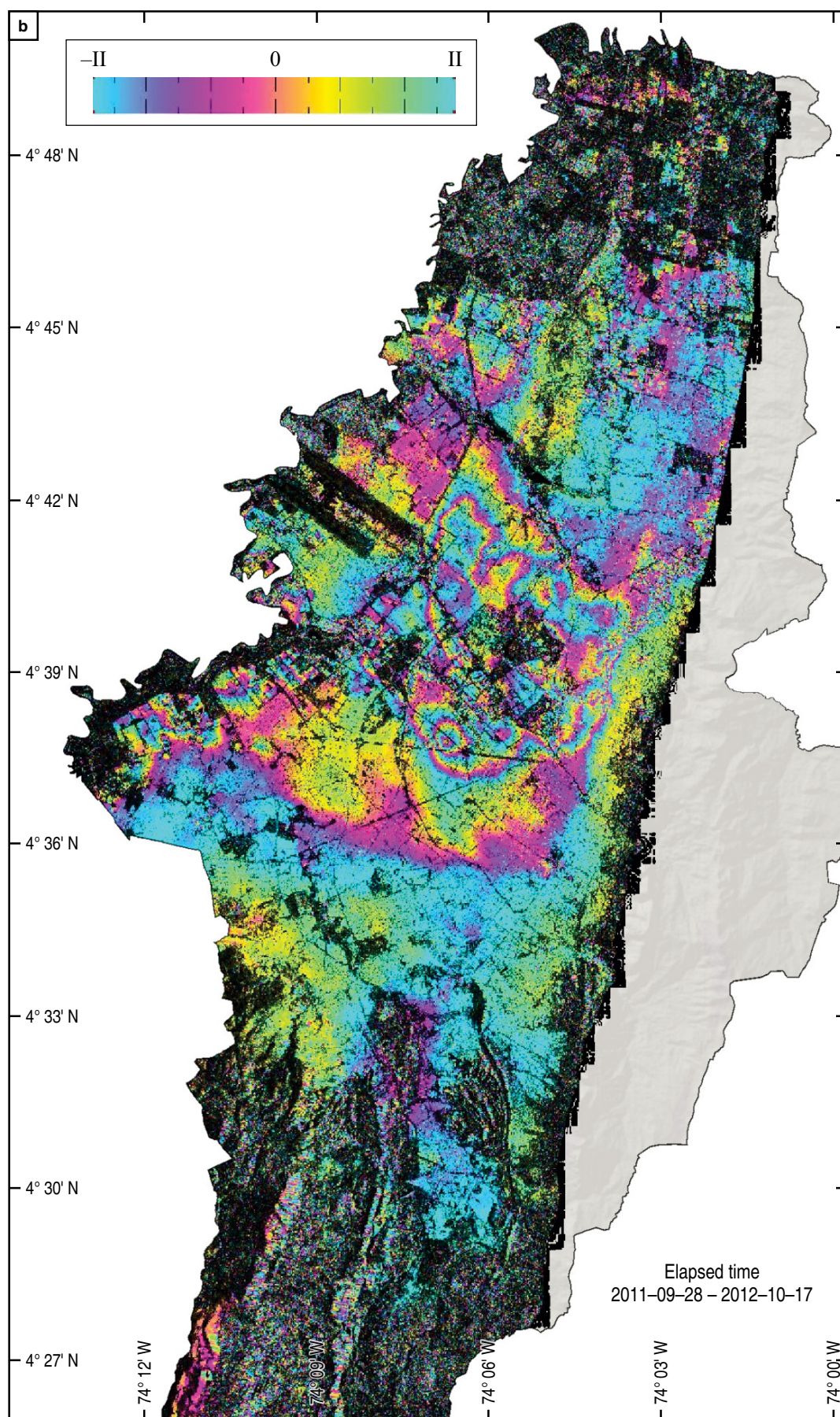
Few GPS permanent stations (cGPS) have been built in the study region, which is also the case for field stations for campaigns. So far, only one cGPS station, the previously mentioned IGS BOGT station, could permit making any comparison with the InSAR results. Four campaigns to gather data from the field stations that are part of the Bogotá GPS Geodetic Network have
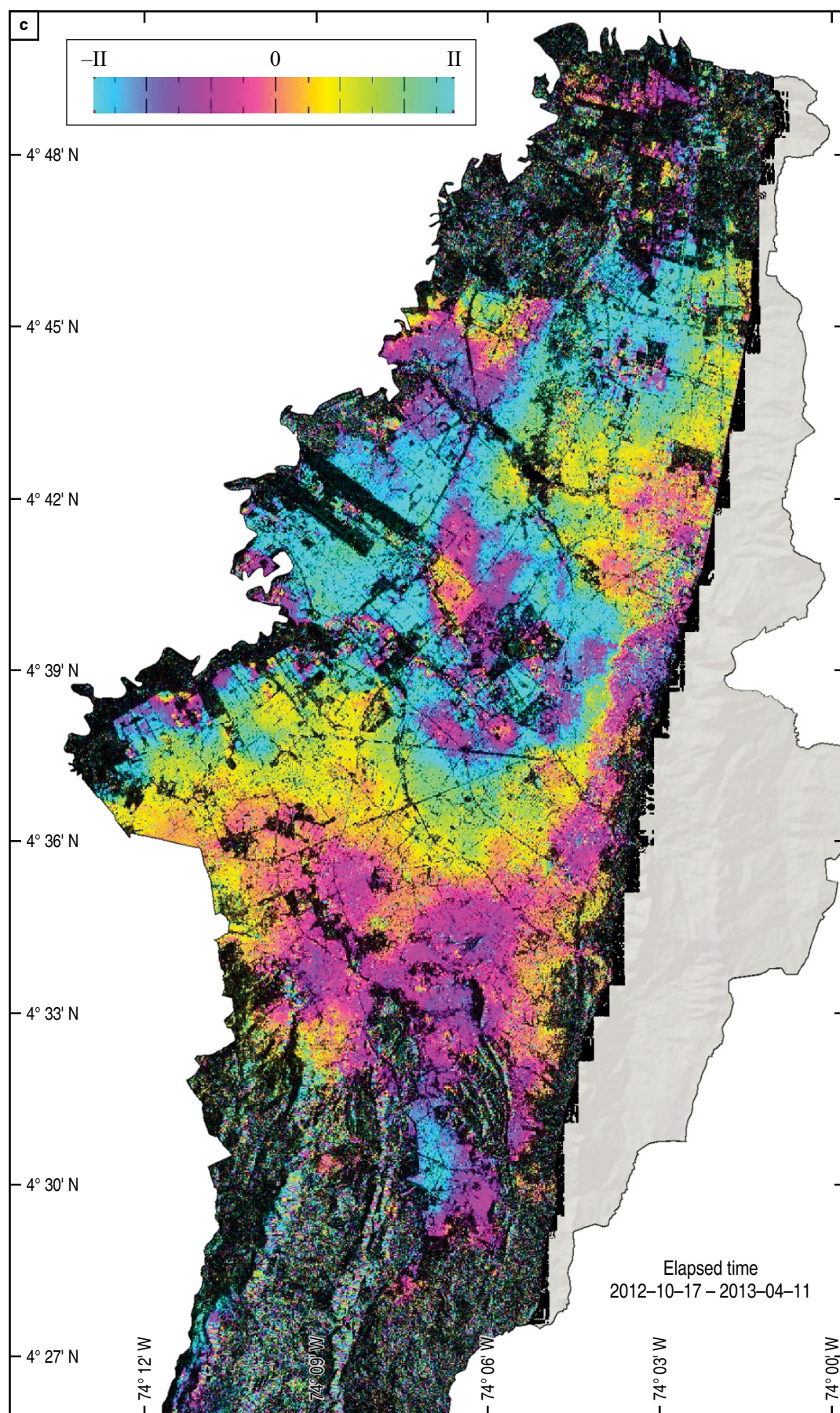
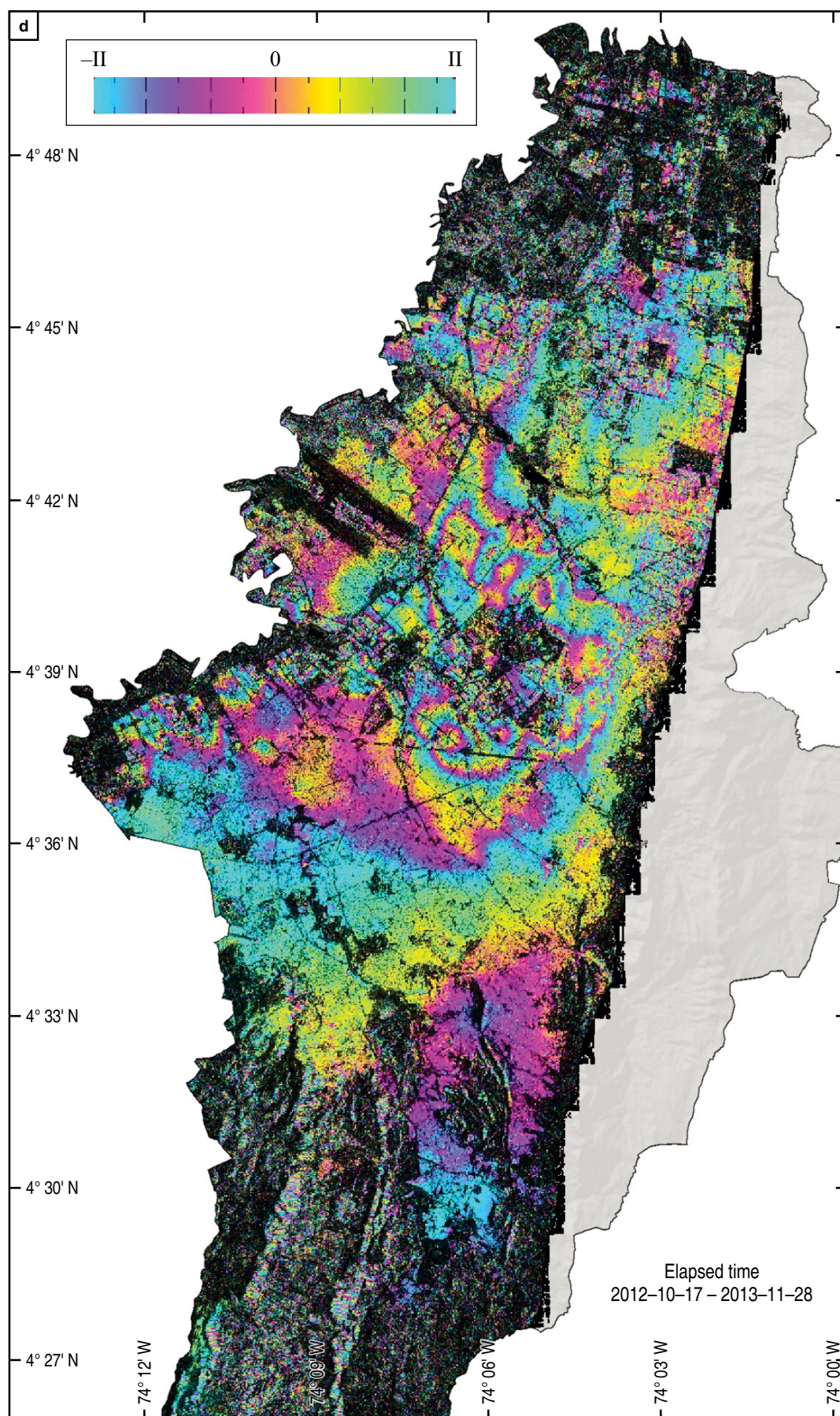**Table 1.** Uncertainties for the three selected sites.

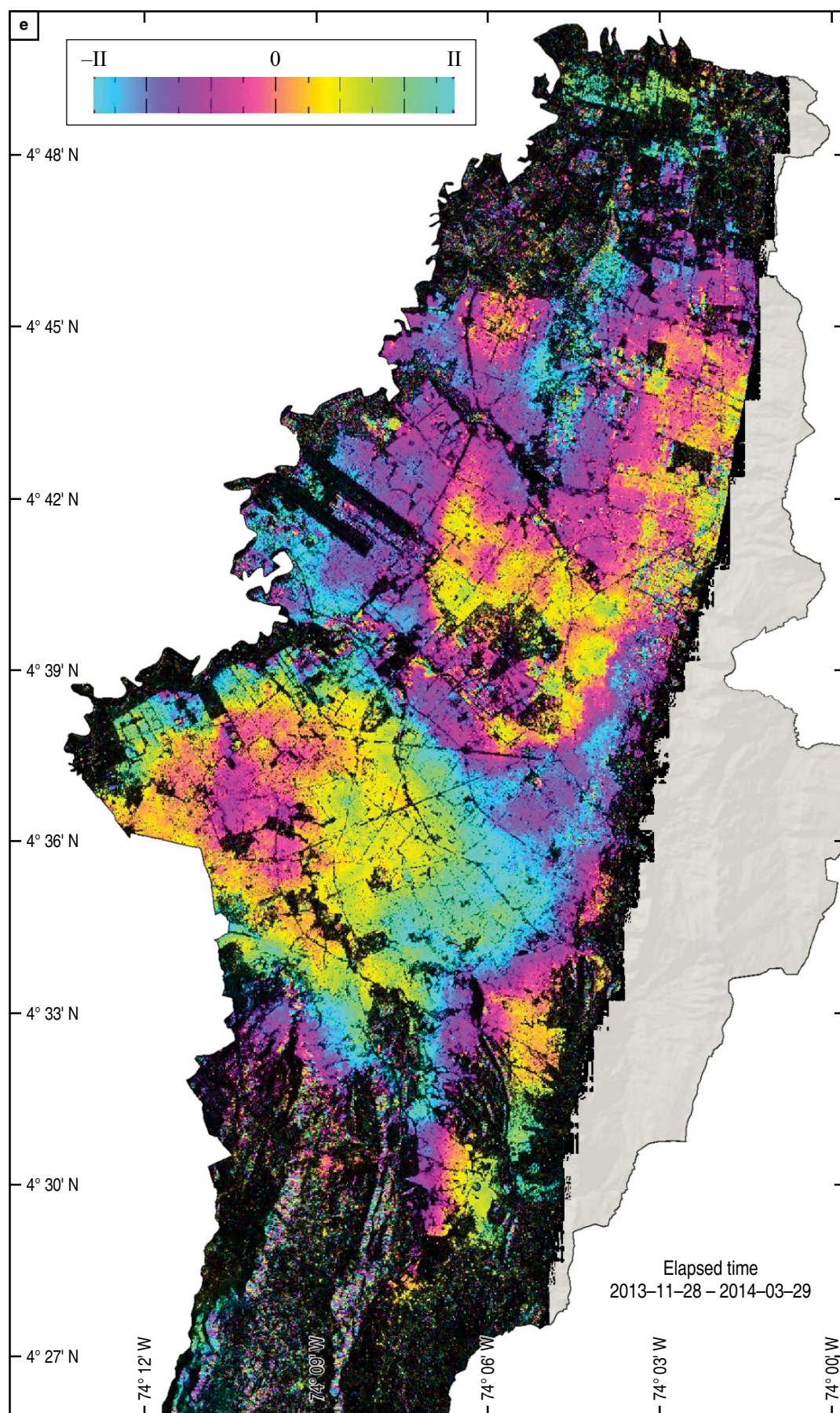| Epoch | Uncertainties (cm) | | | Epoch | Uncertainties (cm) | | |
	Site 1 Puente Aranda	Site 2 Normandía	Site 3 La Guaca		Site 1 Puente Aranda	Site 2 Normandía	Site 3 La Guaca
2011–09–28	0	0	0	2015–01–20	0.13	0.07	0.10
2011–10–09	0.00	0.00	0.00	2015–01–31	0.13	0.07	0.11
2011–10–20	0.00	0.01	0.01	2015–03–05	0.14	0.07	0.12
2011–12–14	0.01	0.03	0.03	2015–03–27	0.14	0.07	0.13
2012–01–05	0.02	0.03	0.03	2015–04–07	0.14	0.06	0.13
2012–01–16	0.02	0.03	0.04	2015–04–29	0.14	0.06	0.13
2012–01–27	0.02	0.04	0.04	2015–05–10	0.14	0.06	0.13
2012–02–07	0.02	0.04	0.04	2015–06–01	0.13	0.06	0.12
2012–02–18	0.02	0.04	0.05	2015–07–04	0.13	0.07	0.10
2012–02–29	0.03	0.04	0.05	2015–08–06	0.13	0.07	0.09
2012–03–11	0.03	0.05	0.05	2015–09–08	0.13	0.07	0.08
2012–04–13	0.03	0.06	0.05	2015–10–11	0.13	0.07	0.07
2012–05–16	0.05	0.08	0.06	2015–11–02	0.13	0.07	0.07
2012–07–21	0.08	0.09	0.05	2015–11–13	0.13	0.07	0.07
2012–08–01	0.08	0.09	0.05	2015–12–05	0.13	0.07	0.07
2012–08–23	0.08	0.08	0.05	2015–12–16	0.13	0.07	0.08
2012–09–03	0.08	0.07	0.04	2016–02–09	0.13	0.07	0.10
2012–09–14	0.07	0.07	0.04	2016–03–02	0.13	0.07	0.12
2012–09–25	0.07	0.07	0.04	2016–04–04	0.14	0.08	0.14
2012–10–17	0.07	0.06	0.04	2016–05–07	0.14	0.08	0.14
2013–04–11	0.12	0.06	0.05	2016–06–09	0.13	0.07	0.12
2013–11–28	0.13	0.08	0.07	2016–07–12	0.13	0.07	0.09
2013–12–09	0.13	0.08	0.07	2016–08–03	0.12	0.07	0.08
2013–12–20	0.13	0.08	0.07	2016–09–05	0.12	0.07	0.07
2014–03–29	0.13	0.07	0.08	2016–10–08	0.12	0.07	0.07
2014–04–20	0.13	0.07	0.08	2016–11–10	0.12	0.08	0.07
2014–05–01	0.13	0.07	0.08	2016–12–13	0.13	0.08	0.07
2014–05–23	0.13	0.08	0.08	2017–01–04	0.14	0.09	0.08
2014–06–03	0.13	0.08	0.08	2017–04–13	0.13	0.08	0.09
2014–06–14	0.13	0.08	0.08	2017–05–27	0.13	0.09	0.09
2014–06–25	0.13	0.08	0.08	2017–06–29	0.13	0.09	0.09
2014–07–17	0.13	0.08	0.08	2017–07–10	0.13	0.09	0.09
2014–07–28	0.13	0.08	0.08	2017–07–21	0.13	0.08	0.09
2014–08–08	0.13	0.08	0.08	2017–08–12	0.13	0.08	0.09
2014–08–19	0.13	0.08	0.08	2017–09–14	0.12	0.08	0.09
2014–11–15	0.13	0.07	0.09	2017–10–17	0.11	0.08	0.09
2014–12–18	0.13	0.07	0.09				

Figure 11. (a–l). Illustration of the sequence of twelve interferograms generated by thirteen images taken at different dates in which the vertical displacements are evident. The subsidence zones in the central zone of Bogotá are clearly visible and represented in interferometric strips, where each color cycle, being band X, corresponds to 1.56 centimeters of relative vertical displacement.
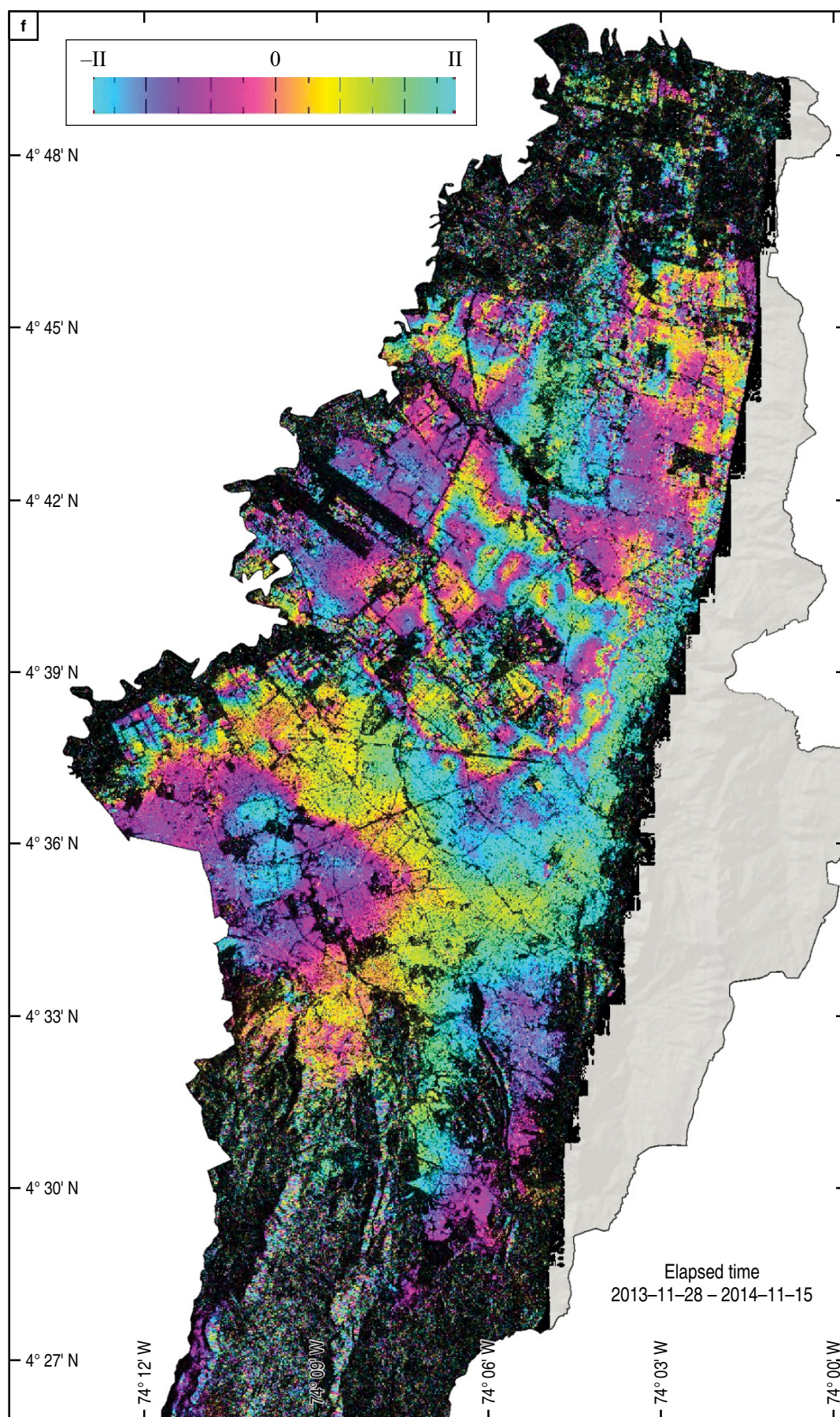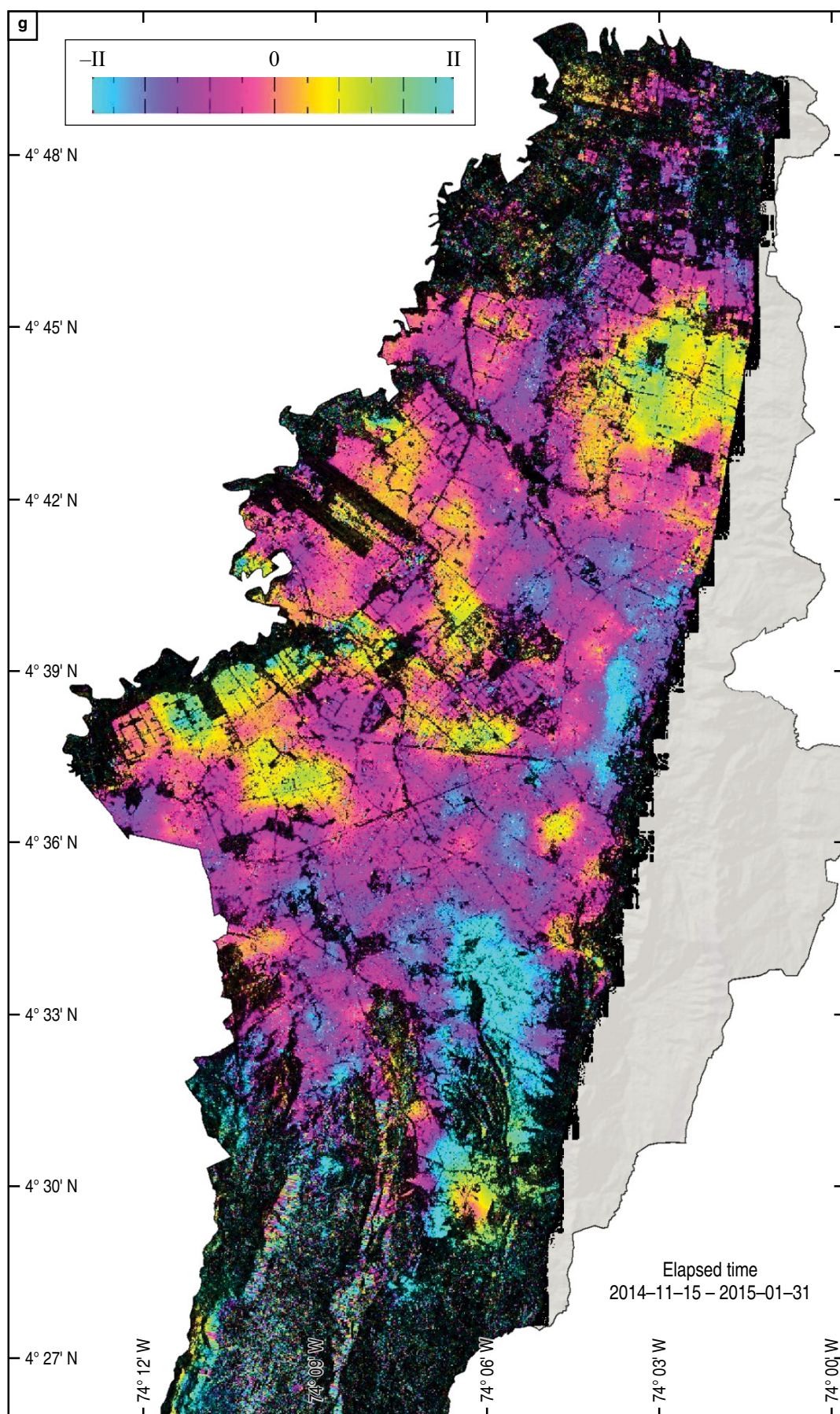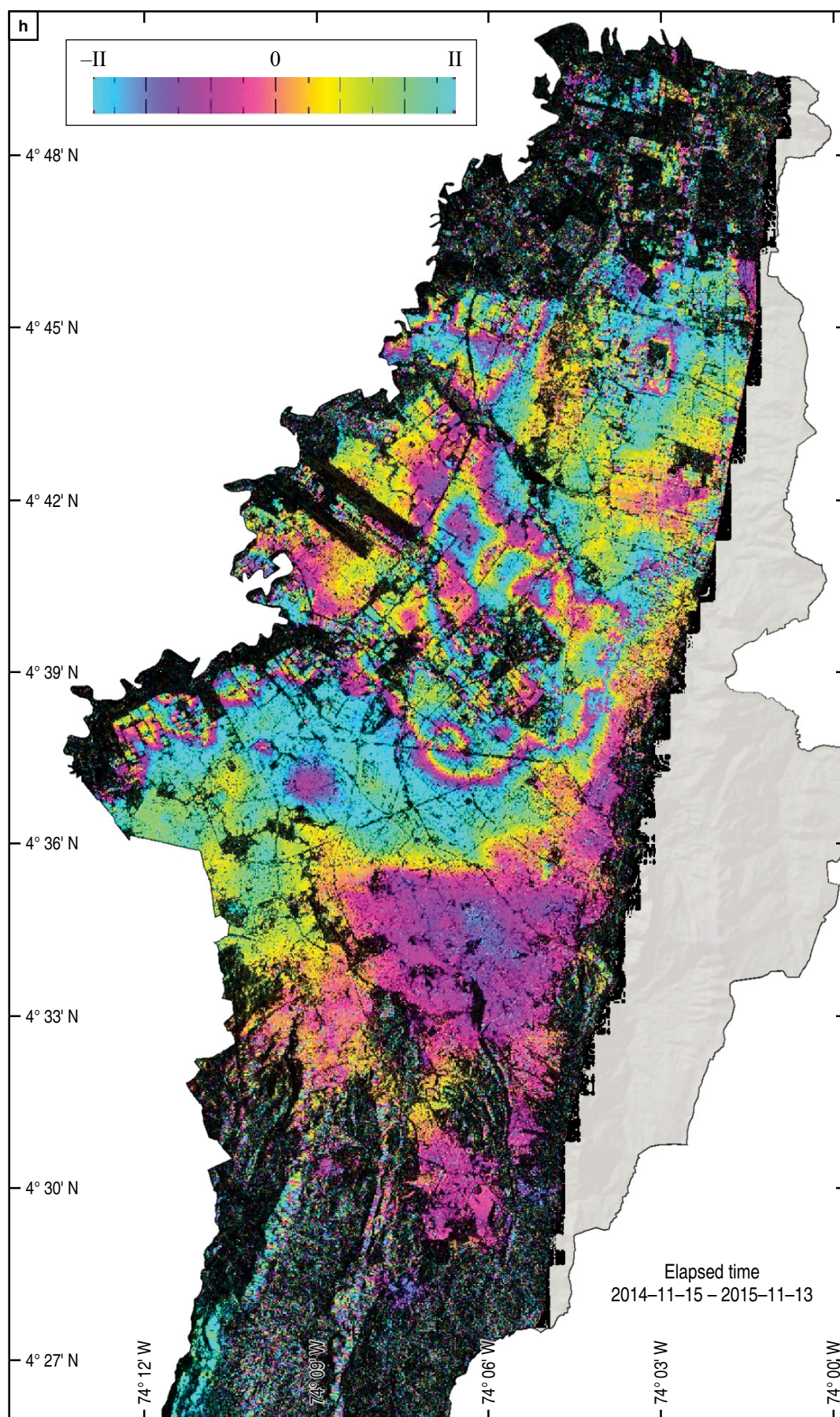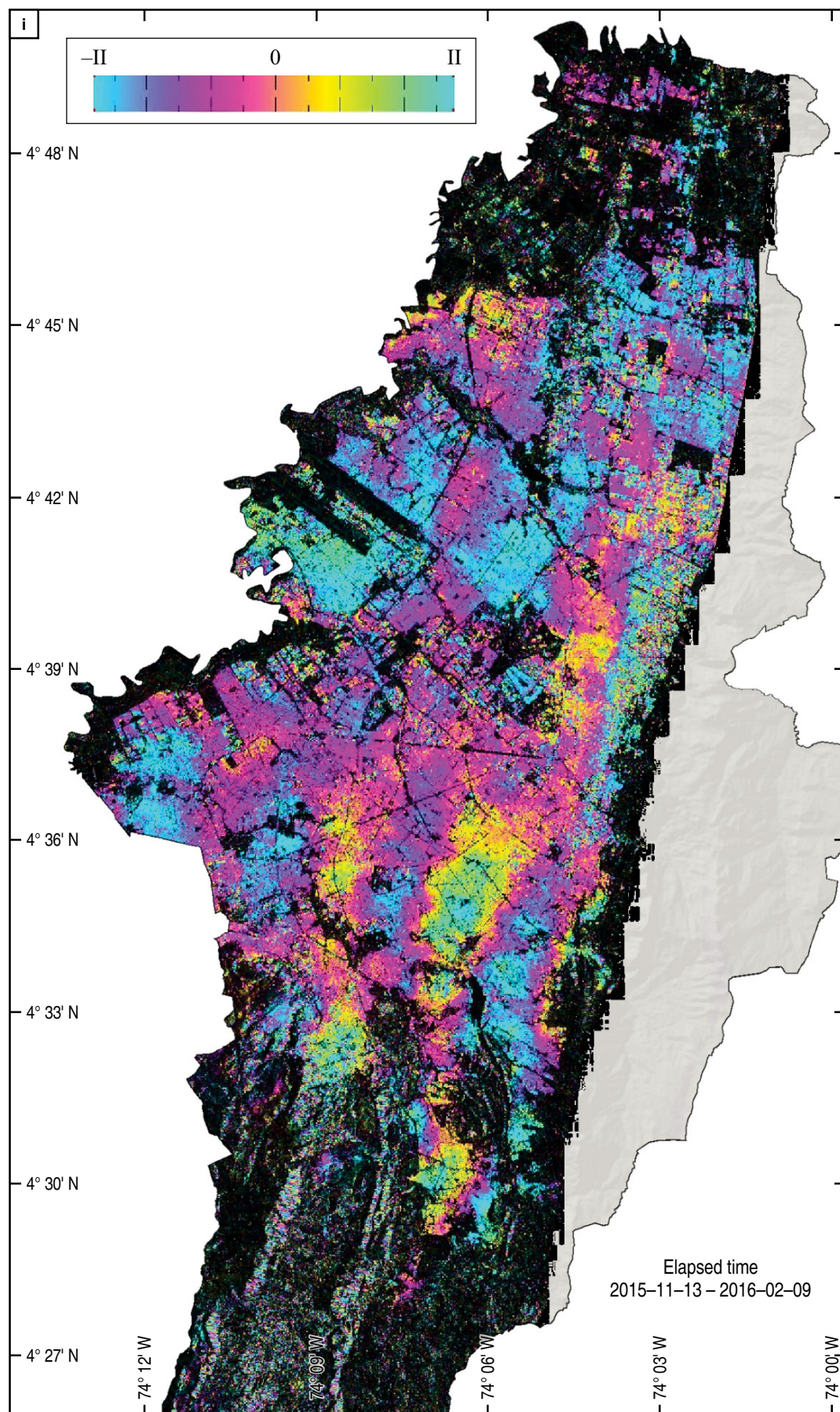
Mapping Land Subsidence in Bogotá, Colombia, Using the Interferometric Synthetic Aperture Radar (InSAR) Technique with TerraSAR–X Images

Quaternary

Elapsed time
2014–11–15 – 2015–01–31

Elapsed time
2016–11–10 – 2017–10–17

Mapping Land Subsidence in Bogotá, Colombia, Using the Interferometric Synthetic Aperture Radar (InSAR) Technique with TerraSAR–X Images
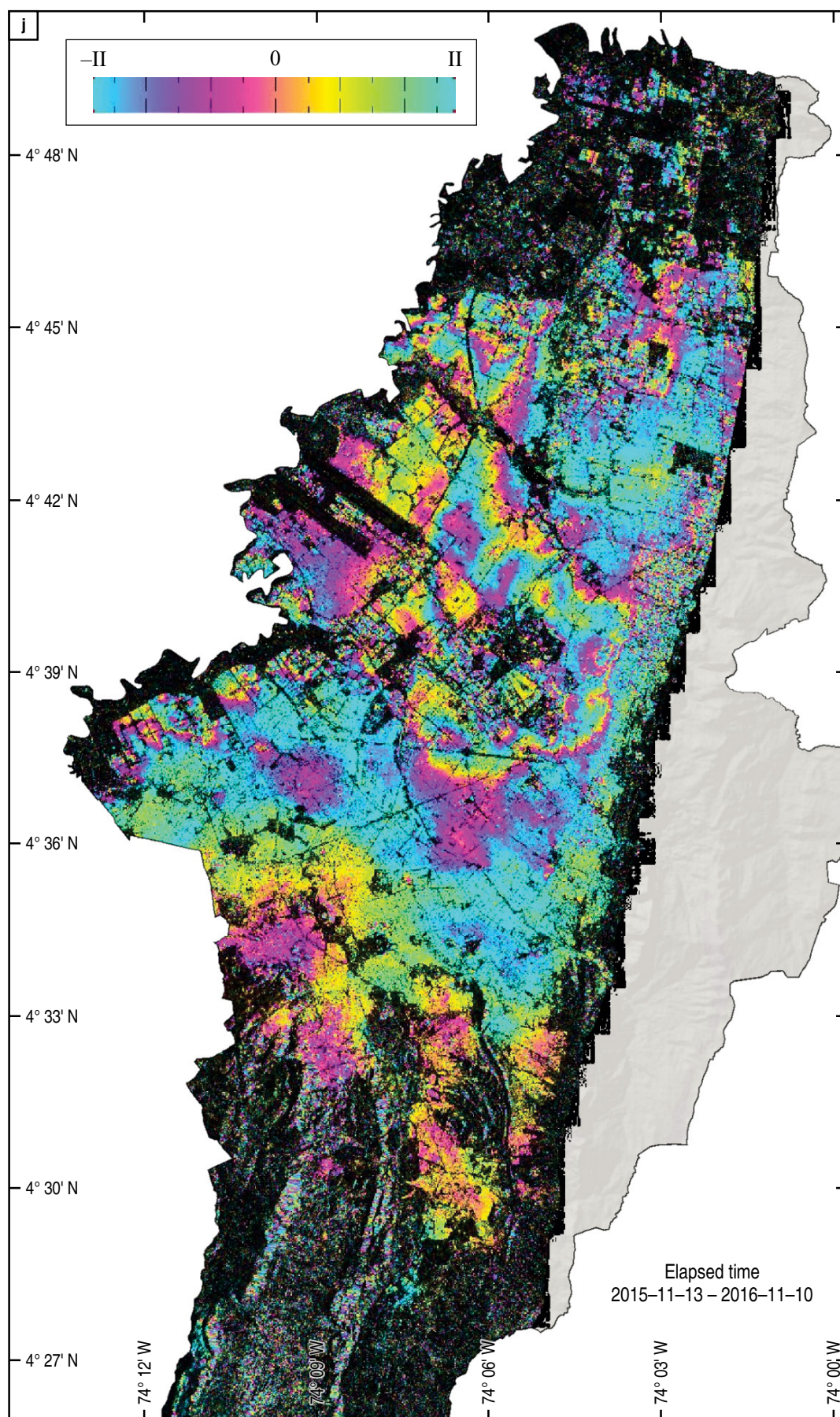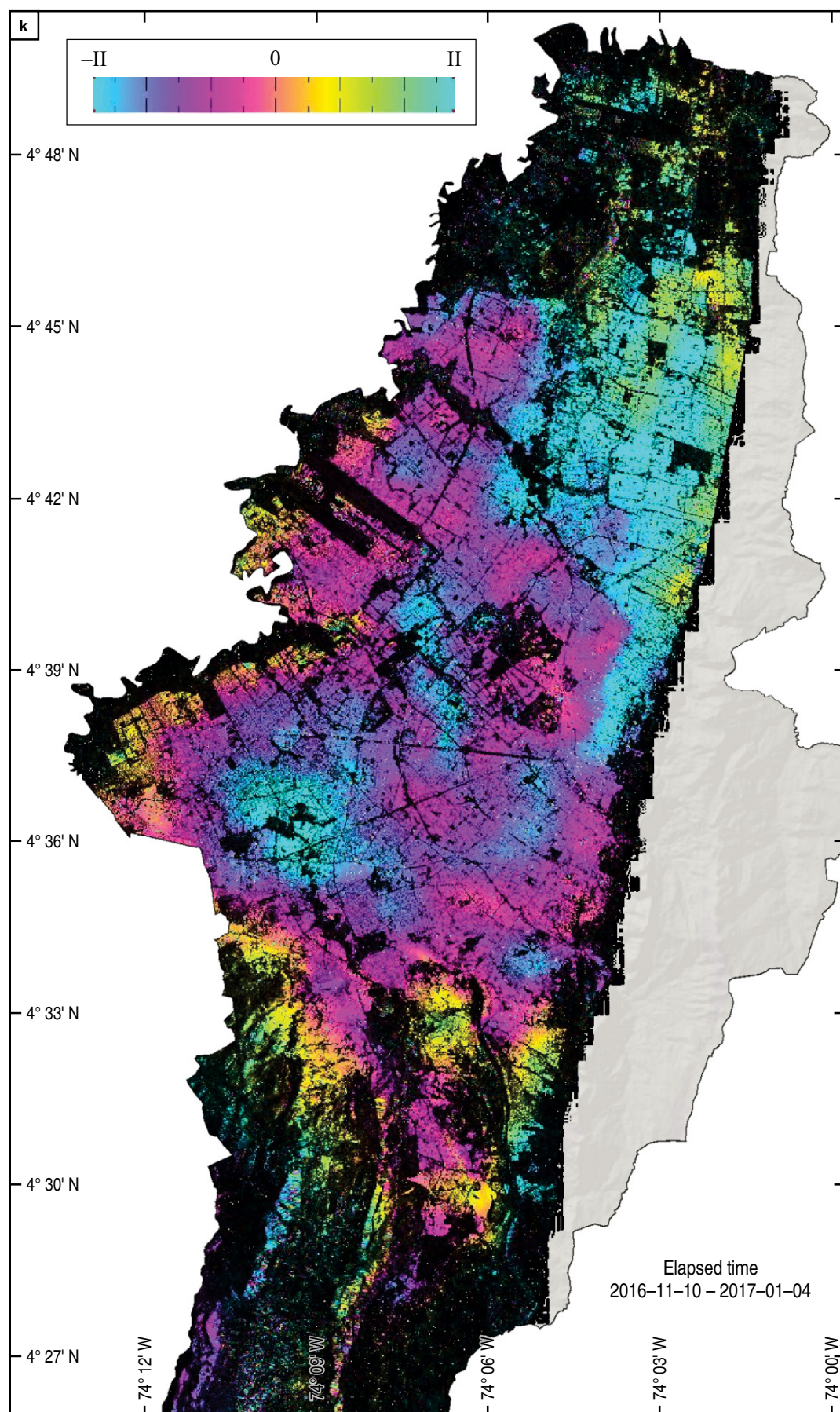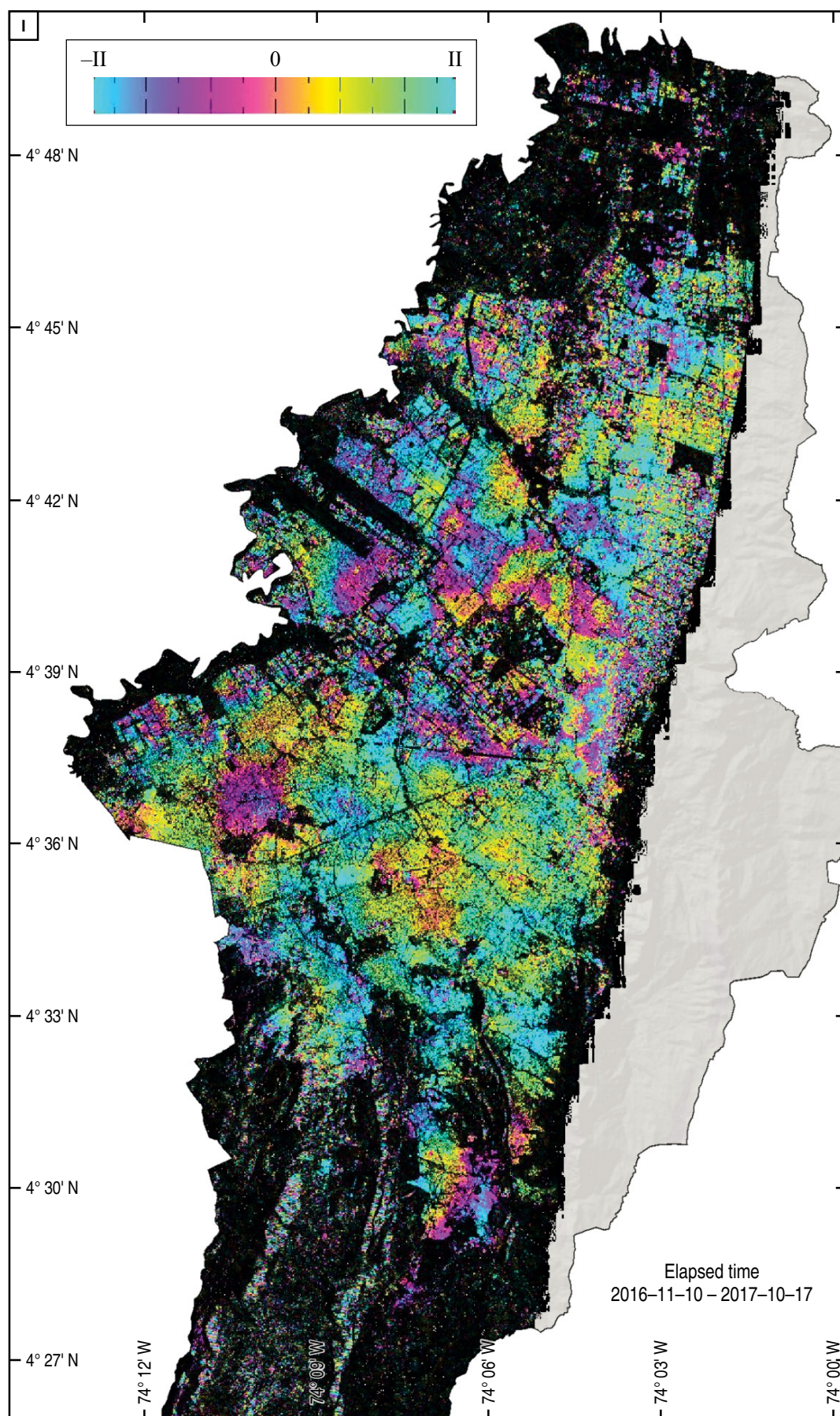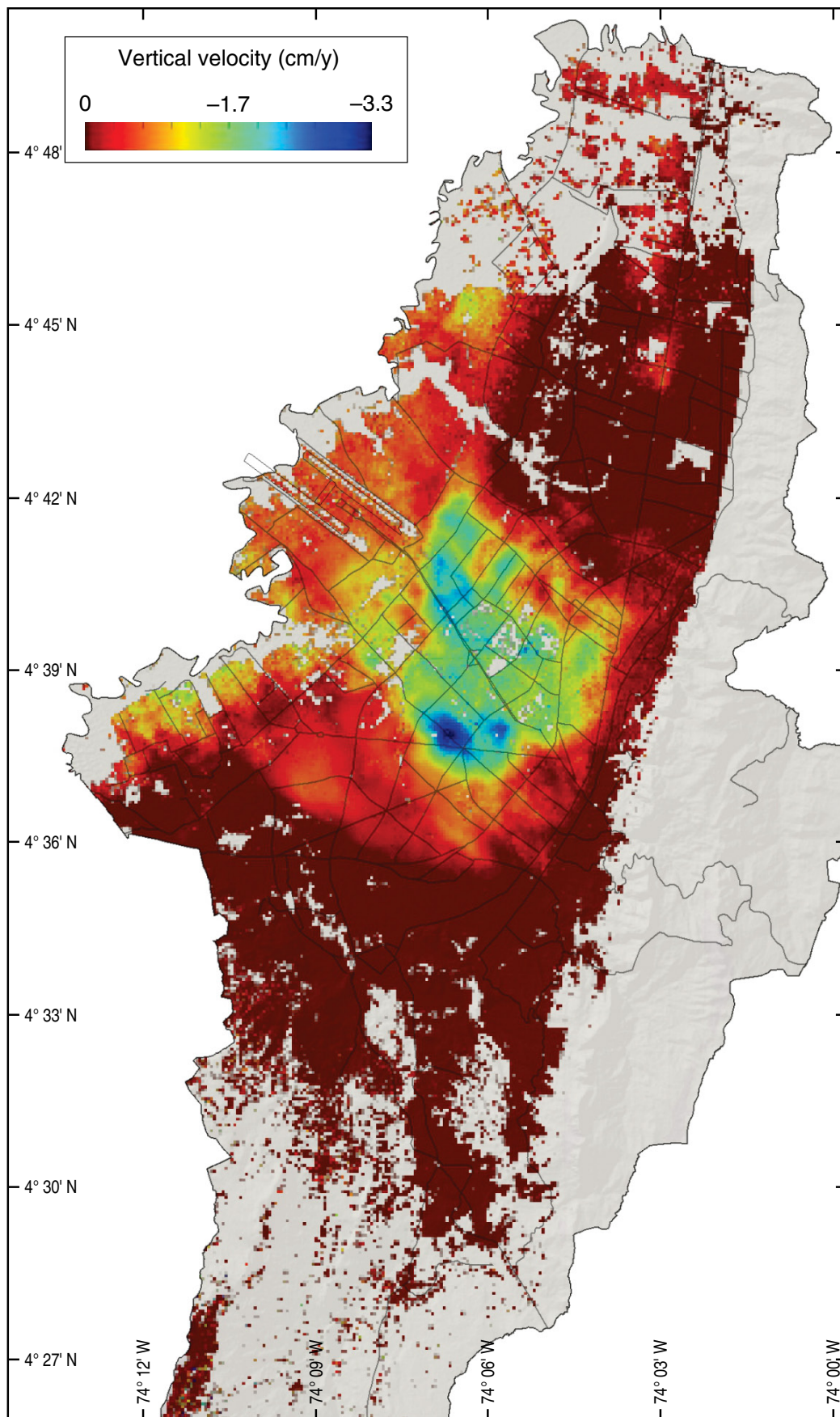
Quaternary

Figure 12. Map of subsidence model for Bogotá, from 28 September 2011 to 17 October 2017, obtained using TerraSAR–X images.
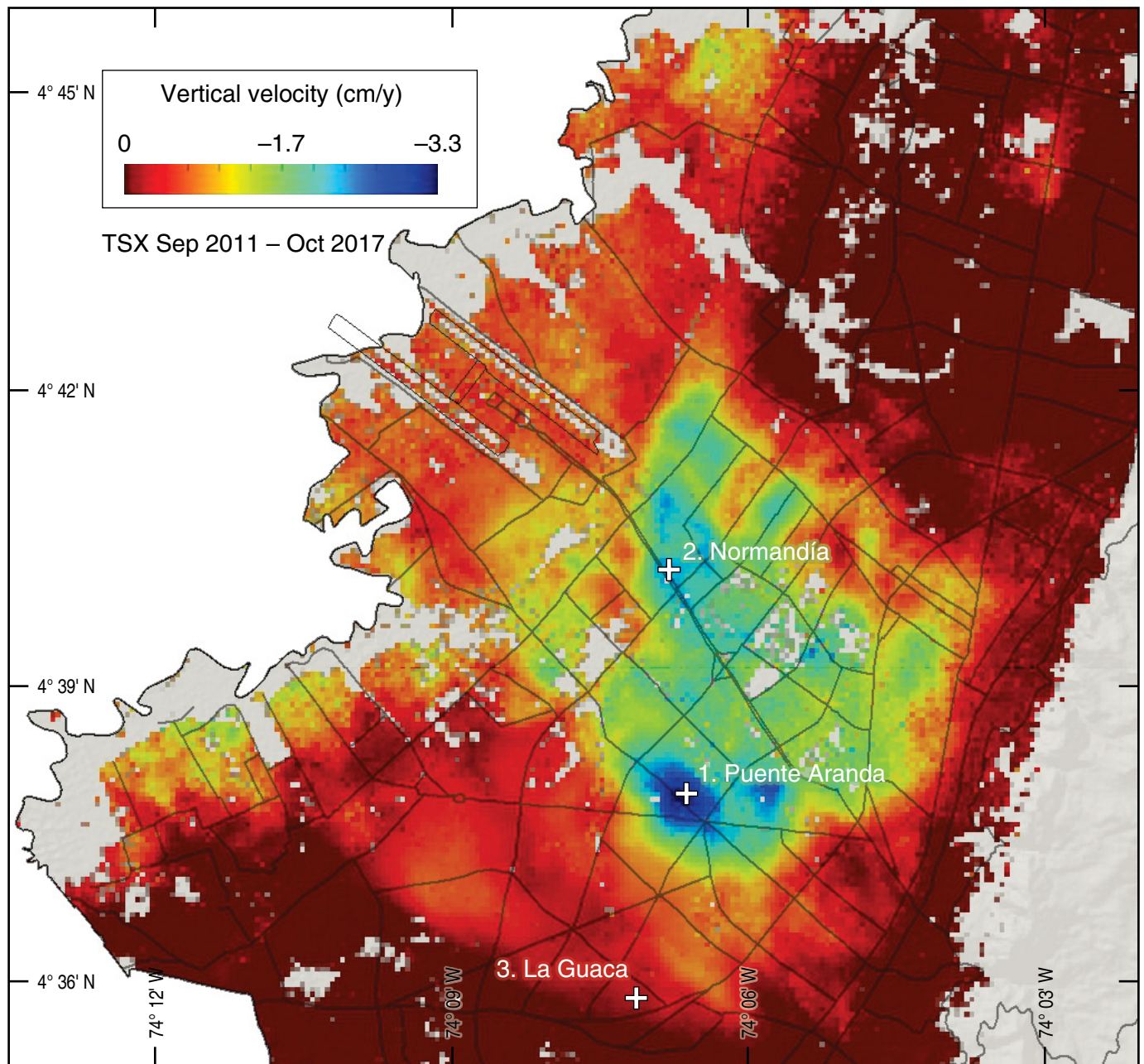
Figure 13. Map of the central area of the Bogotá city in which it is possible to observe a wide zone with scattered patches. Three sites with highest, medium, and low values of subsidence are located on the map.

been performed so far with the support of the Unidad Administrativa Especial de Catastro Distrital of the municipality. To obtain more reliable results from the cGPS stations, it is necessary to get data with at least 2.5 years of observation and to perform more field campaigns.

Various authors have proposed similar arguments regarding the possible causes of the subsidence in Bogotá. The study carried out by the Universidad Nacional de Colombia (2011) summarizes these causes, among which the most important factors are reductions in the depths of groundwater potentiometric levels, superficial drying due to lowering groundwater levels,

effects of vegetation in some places, land overloads due to the weights of buildings, and tectonic effects that can generate land surface variations. Bogotá is a city that has been growing at an accelerated rate, both horizontally and vertically.

A main consideration that must be taken into account in order to gain better knowledge about the land subsidence in the city of Bogotá is to combine InSAR with ground–based measurements such as GPS and to obtain aquifer–related data that would contribute to acquiring high temporal resolutions and the formulation of hydrogeological models. That means that more observation time is necessary to obtain very precise results that
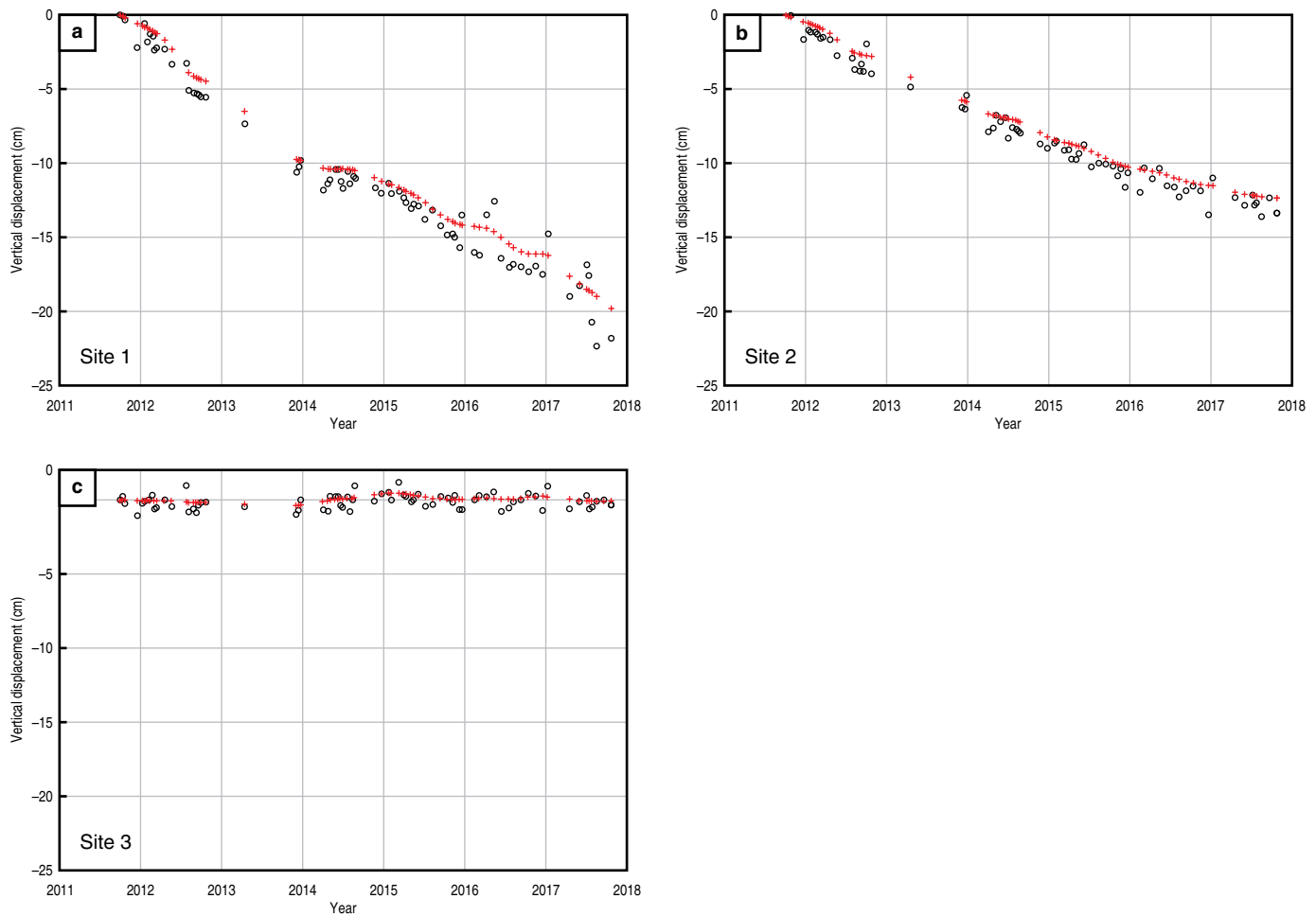
Mapping Land Subsidence in Bogotá, Colombia, Using the Interferometric Synthetic Aperture Radar (InSAR) Technique with TerraSAR–X Images

Quaternary

Figure 14. Time series of the sites located in the central area of the Bogotá city that illustrate the behavior of the subsidence in those sites (highest, medium, and low values, respectively). **(a)** Site 1, **(b)** Site 2, and **(c)** Site 3. Black circles correspond to raw data and red crosses correspond to filtered observations.

will help local authorities adopt the necessary measures to reduce the risks associated with the land subsidence phenomena in Bogotá. In addition, information on ground or building displacement that serves as a key for evaluating the subsidence processes must be acquired. In this way, an interdisciplinary approach focused on research based on relationships between geodetic, geological, geotechnical, and hydrogeological issues and subsidence phenomena must be used and constitutes the main challenge of this project.

For this, it is necessary to continue carrying out these types of studies in general on the entire Sabana de Bogotá and not just for the city of Bogotá. The geodetic results obtained, while spatially restricted, demonstrate the reliability of the techniques used. Therefore, it is important to increase the number of permanent and field GPS stations to expand the spatial coverage of the geodetic network as well as using other types of radar images in the C and L bands of the electromagnetic spectrum to take advantage of the benefits that each offers and thus obtain more data.

Acknowledgments

References

Agram, P., Jolivet, R. & Simons, M. 2012a. The generic InSAR analysis toolbox, user manual. California Institute of Technology, 100 p. Pasadena, USA.

Agram, P.S, Jolivet, R., Riel, B.V., Simons, M., Doin, M.P., Lasserre, M.C. & Hetland, E.A. 2012b. GIAnT–generic InSAR analysis toolbox. American Geophysical Union, Fall Meeting 2012. Abstract id. G43A–0897, 1 p. San Francisco, USA.

Agram, P.S., Jolivet, R., Riel, B.V., Lin, Y.N., Simons, M., Hetland, E., Doin, M.P. & Lasserre, C. 2013. New radar interferometric time series analysis toolbox released. EOS, Transactions American Geophysical Union, 94(7): 69–70. https://doi.org/10.1002/2013EO070001

Agram, P.S., Gurrola, E.M., Lavalle, M., Sacco, G.F. & Rosen, P.A. 2016. The InSAR Scientific Computing Environment (ISCE): An earth science SAR processing framework, toolbox, and foundry. American Geophysical Union, Fall Meeting 2016. Abstract #G43A–1039, 1 p. San Francisco, USA.

Aly, M.H., Zebker, H.A., Giardino, J.R. & Klein, A.G. 2009. Permanent scatterer investigation of land subsidence in Greater Cairo, Egypt. Geophysical Journal International, 178(3): 1238–1245. https://doi.org/10.1111/j.1365-246X.2009.04250.x

Amelung, F., Galloway, D.L., Bell, J.W., Zebker, H.A. & Laczniak, R.J. 1999. Sensing the ups and downs of Las Vegas: InSAR reveals structural control of land subsidence and aquifer–system deformation. Geology, 27(6): 483–486. https://doi.org/10.1130/0091-7613(1999)027<0483:STUADO>2.3.CO;2

Antonio–Fragala, F. & Obregón–Neira, N. 2011. Estimación de la recarga media anual en los acuíferos de la Sabana de Bogotá. Ingeniería y Universidad, 15(1): 145–169.

Arbeláez, A.M., Steiner, R., Becerra, A. & Wills, D. 2011. Housing tenure and housing demand in Colombia. IDB Working Paper, Series 259, 50 p.

Arbinger, C., D'Amico, S. & Eineder, M. 2004. Precise ground–in–the–loop orbit control for low earth observation satellites. 18th International Symposium on Space Flight Dynamics Proceedings (ESA SP–548), p. 333. Munich, Germany.

Bawden, G.W., Thatcher, W., Stein, R.S., Hudnut, K.W. & Peltzer, G. 2001. Tectonic contraction across Los Angeles after removal of groundwater pumping effects. Nature, 412(6849): 812–815. https://doi.org/10.1038/35090558

Bayuaji, L., Sumantyo, J.T.S. & Kuze, H. 2010. ALOS PALSAR D–InSAR for land subsidence mapping in Jakarta, Indonesia. Canadian Journal of Remote Sensing, 36(1): 1–8. https://doi.org/10.5589/m10-023

Berardino, P., Fornaro, G., Lanari, R. & Sansosti, E. 2002. A new algorithm for surface deformation monitoring based on small baseline differential SAR interferograms. IEEE Transactions on Geoscience and Remote Sensing, 40(11): 2375–2383. https://doi.org/10.1109/TGRS.2002.803792

Bertiger, W., Desai, S.D., Haines, B., Harvey, N., Moore, A.W., Owen, S. & Weiss, J.P. 2010. Single receiver phase ambiguity resolution with GPS data. Journal of Geodesy, 84(5): 327–337. https://doi.org/10.1007/s00190-010-0371-9

Bock, Y., Wdowinski, S., Ferretti, A., Novali, F. & Fumagalli, A. 2012. Recent subsidence of the Venice Lagoon from continuous GPS and interferometric synthetic aperture radar. Geochemistry, Geophysics, Geosystems, 13(3): 1–13. https://doi.org/10.1029/2011GC003976

Bos, M.S., Fernandes, R.M.S., Williams, S.D.P. & Bastos, L. 2013. Fast error analysis of continuous GNSS observations with missing data. Journal of Geodesy, 87(4): 351–360. https://doi.org/10.1007/s00190-012-0605-0

Bozzano, F., Esposito, C., Franchi, S., Mazzanti, P., Perissin, D., Rocca, A. & Romano, E. 2015. Understanding the subsidence process of a Quaternary plain by combining geological and hydrogeological modelling with satellite InSAR data: The Acque Albule Plain case study. Remote Sensing of Environment, 168: 219–238. https://doi.org/10.1016/j.rse.2015.07.010

Burbey, T.J. 2002. The influence of faults in basin–fill deposits on land subsidence, Las Vegas Valley, Nevada, USA. Hydrogeology Journal, 10(5): 525–538. https://doi.org/10.1007/s10040-002-0215-7

Bürgmann, R., Rosen, P.A. & Fielding, E.J. 2000. Synthetic aperture radar interferometry to measure Earth's surface topography and its deformation. Annual Review of Earth and Planetary Sciences, 28(1): 169–209. https://doi.org/10.1146/annurev.earth.28.1.169

Cabral–Cano, E., Dixon, T.H., Miralles–Wilhelm, F., Díaz–Molina, O., Sánchez–Zamora, O. & Carande, R.E. 2008. Space geodetic imaging of rapid ground subsidence in Mexico City. GSA Bulletin, 120(11–12): 1556–1566. https://doi.org/10.1130/B26001.1

Carvajal, J.H. & Navas, O. 2016. Bogotá "Savanna". In: Hermelin, M. (editor), Landscapes and landforms of Colombia. Springer, p. 115–126. https://doi.org/10.1007/978-3-319-11800-0_10

Chaussard, E., Amelung, F., Abidin, H. & Hong, S.H. 2013. Sinking cities in Indonesia: ALOS PALSAR detects rapid subsidence due to groundwater and gas extraction. Remote Sensing of Environment, 128: 150–161. https://doi.org/10.1016/j.rse.2012.10.015

Chaussard, E., Wdowinski, S., Cabral–Cano, E. & Amelung, F. 2014. Land subsidence in central Mexico detected by ALOS InSAR time–series. Remote Sensing of Environment, 140: 94–106. https://doi.org/10.1016/j.rse.2013.08.038

Corapcioglu, M.Y. 1984. Land subsidence: A state–of–the–art review. In: Bear, J. & Corapcioglu, M.Y. (editors), Fundamentals of transport phenomena in porous media. NATO ASI, Series 82, Martinus Nijhoff Publishers, p. 369–444. Dordrecht, the Netherlands. https://doi.org/10.1007/978-94-009-6175-3_8

Damoah–Afari, P., Ding, X., Li, Z., Lu, Z. & Omura, M. 2007. Six years of land subsidence in Shanghai revealed by JERS–1 SAR data. IEEE International Geoscience and Remote Sensing Symposium. Abstracts, p. 2093–2097. Barcelona, Spain. https://doi.org/10.1109/IGARSS.2007.4423246

Departamento Administrativo del Medio Ambiente. 1999. Elaboración del modelo hidrogeológico para los acuíferos de Santafé de Bogotá D.C. DAMA–PNUD–Hidrogeocol, 45 p. Bogotá.

Mapping Land Subsidence in Bogotá, Colombia, Using the Interferometric Synthetic Aperture Radar (InSAR) Technique with TerraSAR–X Images

Quaternary

Departamento Administrativo Nacional de Estadística. 2020. Resultados Censo Nacional de Población y Vivienda. 2018. https://www.dane.gov.co/index.php/estadisticas-por-tema/demografia-y-poblacion/censo-nacional-de-poblacion-y-vivenda-2018 (consulted in July 2020).

Deutsches Zentrum für Luft– und Raumfahrt. 2009. TerraSAR–X: The German radar eye in space. 44 p. Bonn, Germany.

Dixon, T.H., Amelung, F., Ferretti, A., Novali, F., Rocca, F., Dokka, R., Sella, G., Kim, S.W., Wdowinski, S. & Whitman, D. 2006. Subsidence and flooding in New Orleans. Nature, 441(7093): 587–588. https://doi.org/10.1038/441587a

Doin, M.P., Lodge, F., Guillaso, S., Jolivet, R., Lasserre, C., Ducret, G., Grandin, R., Pathier, E. & Pinet, V. 2011. Presentation of the small baseline NSBAS processing chain on a case example: The Etna deformation monitoring from 2003 to 2010 using ENVISAT data. FRINGE Symposium 2011, Proceedings, 7 p. Frascati, Italy.

Eineder, M., Runge, H., Boerner, E., Bamler, R., Adam, N., Schättler, B., Breit, H. & Suchandt, S. 2003. SAR interferometry with TerraSAR–X. FRINGE Workshop 2003, Proceedings, 6 p. Frascati, Italy.

European Space Agency. 2014. The ASAR user guide, ESA earthnet online. https://earth.esa.int/handbooks/asar/CNTR1.html#eph.asar.ug (consulted in October 2018).

Fergason, K.C., Rucker, M.L. & Panda, B.B. 2015. Methods for monitoring land subsidence and earth fissures in the Western USA. Proceedings of the International Association of Hydrological Sciences, 372: 61–366. https://doi.org/10.5194/piahs-372-361-2015

Ferreti, A., Monti–Guarnieri, A., Prati, C., Rocca, F. & Massonnet, D. 2007. InSAR principles: Guidelines for SAR interferometry processing and interpretation. ESA Publications, TM–19, 48 p. The Netherlands.

Fruneau, B. & Sarti, F. 2000. Detection of ground subsidence in the city of Paris using radar interferometry: Isolation of deformation from atmospheric artifacts using correlation. Geophysical Research Letters, 27(24): 3981–3984. https://doi.org/10.1029/2000GL008489

Fruneau, B., Deffontaines, B., Rudant, J.P. & Le Parmentier, A.M. 2005. Monitoring vertical deformation due to water pumping in the city of Paris (France) with differential interferometry. Comptes Rendus Geoscience, 337(13): 1173–1183. https://doi.org/10.1016/j.crte.2005.05.014

Global Volcanism Program. 2012. Report on Mauna Loa (United States). In: Wunderman, R. (editor), Bulletin of the Global Volcanism Network, 37: 5. Smithsonian Institution. https://doi.org/10.5479/si.GVP.BGVN201205-332020

Goldstein, R.M., Zebker, H.A. & Werner, C.L. 1988. Satellite radar interferometry: Two–dimensional phase unwrapping. Radio Science, 23(4): 713–720. https://doi.org/10.1029/RS023i004p00713

Gurrola, E., Rosen, P., Sacco, G., Szeliga, W., Zebker, H., Simons, M., Sandwell, D., Shanker, P., Wortham, C. & Chen, A. 2010. InSAR scientific computing environment. American Geophysical Union Meeting. Abstract id. IN43B–1397. San Francisco, USA.

Heleno, S.I.N., Oliveira, L.G.S., Henriques, M.J., Falcão, A.P., Lima, J.N.P., Cooksley, G., Ferretti, A., Fonseca, A.M., Lobo–Ferreira, J.P. & Fonseca, J.F.B.D. 2011. Persistent scatterers interferometry detects and measures ground subsidence in Lisbon. Remote Sensing of Environment, 115(8): 2152–2167. https://doi.org/10.1016/j.rse.2011.04.021

Hoffmann, J., Zebker, H.A., Galloway, D.L. & Amelung, F. 2001. Seasonal subsidence and rebound in Las Vegas Valley, Nevada, observed by synthetic aperture radar interferometry. Water Resources Research, 37(6): 1551–1566. https://doi.org/10.1029/2000WR900404

Hooper, A. & Zebker, H.A. 2007. Phase unwrapping in three dimensions with application to InSAR time series. Journal of the Optical Society of America A, 24(9): 2737–2747. https://doi.org/10.1364/JOSAA.24.002737

Instituto Cartográfico de Cataluña. 2007. Estudio interferométrico diferencial SAR (DInSAR) para la monitorización de deformaciones del terreno en la ciudad de Bogotá. Fondo de Prevención y Atención de Emergencias de Bogotá D.C. Internal report, 28 p. Barcelona, Spain.

Instituto Cartográfico de Cataluña. 2009. Estudios de subsidencias sobre Bogotá mediante técnicas DInSAR. Fondo de Prevención y Atención de Emergencias de Bogotá D.C. Internal report, 26 p. Barcelona, Spain.

Instituto Cartográfico y Geológico de Cataluña. 2014. Análisis de subsidencias mediante DInSAR, análisis de subsidencias mediante técnicas DInSAR. Zona de Bogotá. Fondo de Prevención y Atención de Emergencias de Bogotá D.C. Internal report, 108 p. Barcelona, Spain.

Kahle, R. & D'Amico, S. 2014. The TerraSAR–X precise orbit control: Concept and flight results. International Symposium on Space Flight Dynamics (ISSFD). Conference paper, 12 p. Laurel, USA.

Kaniuth, K., Häfele, P. & Sánchez, L. 2001. Subsidence of the permanent GPS station Bogotá. In: Drewes, H., Dodson, A., Fortes, L.P.S., Sánchez, L. & Sandoval, P. (editors), Vertical reference systems. International Association of Geodesy Symposia, 24, p. 56–59. Berlin–Heidelberg, Germany. https://doi.org/10.1007/978-3-662-04683-8_12

Lanari, R., Mora, O., Manunta, M., Mallorqui, J.J., Berardino, P. & Sansosti, E. 2004. A small–baseline approach for investigating deformations on full–resolution differential SAR interferograms. IEEE Transactions on Geoscience and Remote Sensing, 42(7): 1377–1386. https://doi.org/10.1109/TGRS.2004.828196

Le, T.S., Chang, C.P., Nguyen, X.T. & Yokha, A. 2016. TerraSAR–X data for high–precision land subsidence monitoring: A case

study in the historical centre of Hanoi, Vietnam. Remote Sens, 8(4): 1–23. https://doi.org/10.3390/rs8040338

Lobo–Guerrero, A. 1992. Geología e hidrogeología de Santafé de Bogotá y su sabana. VII Jornadas Geotécnicas de la Ingeniería de Colombia–I Foro sobre Geotecnia de la Sabana de Bogotá. Sociedad Colombiana de Ingenieros–Sociedad Colombiana de Geotecnia, Memoirs II, p. 16–36. Bogotá.

Lobo–Guerrero, A. 1995. Descenso de niveles de agua subterránea en la Sabana de Bogotá. VIII Jornadas Geotécnicas de la Ingeniería de Colombia–II Foro sobre Geotecnia de la Sabana de Bogotá. Sociedad Colombiana de Ingenieros–Sociedad Colombiana de Geotecnia, 11 p. Bogotá.

Lobo–Guerrero, A. 2003. Effects of aquifer overexploitation on the surface infrastructure in the Bogotá Sabana, Colombia. RMZ Materials and Geoenvironment, 50(1): 193–196.

Lobo–Guerrero, A. & Gilboa, Y. 1987. Groundwater in Colombia. Hydrological Sciences Journal, 32(2): 161–178. https://doi.org/10.1080/02626668709491175

López–Quiroz, P., Doin, M.P., Tupin, F., Briole, P. & Nicolás, J.M. 2009. Time series analysis of Mexico City subsidence constrained by radar interferometry. Journal of Applied Geophysics, 69(1): 1–15. https://doi.org/10.1016/j.jappgeo.2009.02.006

Massonnet, D. & Souyris, J.C. 2008. Imaging with synthetic aperture radar. EPFL Press. First Edition, 280 p. Boca Ratón, USA.

Meckel, T.A. 2008. An attempt to reconcile subsidence rates determined from various techniques in southern Louisiana. Quaternary Science Reviews, 27(15–16): 1517–1522. https://doi.org/10.1016/j.quascirev.2008.04.013

Mora–Páez H., 2006. "Red Nacional de Estaciones Geodésicas Satelitales GPS para estudios e investigaciones geodinámicas". Documento BPIN y Fichas de Proyecto, MGA para Departamento Nacional de Planeación. Ingeominas, 63 p. Bogotá.

Mora–Páez, H., Chaussard, E., Wdowinski, S. & Cabral, E. 2013. Space geodetic techniques for assessing land subsidence in Bogota city. XIV Congreso Colombiano de Geología y Primer Simposio de Exploradores. Abstract, p. 83. Bogotá.

Mora–Páez, H., Peláez–Gaviria, J.R., Diederix, H., Bohórquez–Orozco, O., Cardona–Piedrahita, L., Corchuelo–Cuervo, Y., Ramírez–Cadena, J. & Díaz–Mila, F. 2018. Space geodesy infrastructure in Colombia for geodynamics research. Seismological Research Letters, 89(2A): 446–451. https://doi.org/10.1785/0220170185

Mora–Páez, H., Kellogg, J.N. & Freymueller, J.T. 2020. Contributions of space geodesy for geodynamic studies in Colombia: 1988 to 2017. In: Gómez, J. & Pinilla–Pachon, A.O. (editors), The Geology of Colombia, Volume 4 Quaternary. Servicio Geológico Colombiano, Publicaciones Geológicas Especiales 38, p. 479–498. Bogotá. https://doi.org/10.32685/pub.esp.38.2019.14

Muntendam–Bos, A.G., Kleuskens, M.H.P., Bakr, M., De Lange, G. & Fokker, P.A. 2009. Unraveling shallow causes of subsidence. Geophysical Research Letters, 36(10): 1–4. https://doi.org/10.1029/2009GL037190

Ojeda, J. & Donelly, L. 2006. Landslides in Colombia and their impact on towns and cities. 10th IAEG International Congress, Proceedings paper 112, 13 p. Nottinghan, UK.

Osmanoğlu, B., Dixon, T.H., Wdowinski, S., Cabral–Cano, E. & Jiang, Y. 2011. Mexico City subsidence observed with persistent scatterer InSAR. International Journal of Applied Earth Observation and Geoinformation, 13(1): 1–12. https://doi.org/10.1016/j.jag.2010.05.009

Poland, J.F. 1984. Guidebook to studies of land subsidence due to ground–water withdrawal. International Hydrological Programme. Working Group 8.4, UNESCO, 305 p. Chelsea, USA.

Poland, J.F., Lofgren, B.E. & Riley, F.S. 1972. Glossary of selected terms useful in studies of the mechanics of aquifer systems and land subsidence due to fluid withdrawal. Geological Survey Water–Supply Paper 2025, 9 p. Washington, USA. https://doi.org/10.3133/wsp2025

Raucoules, D., Colesanti, C. & Carnec, C. 2007. Use of SAR interferometry for detecting and assessing ground subsidence. Comptes Rendus Geoscience, 339(5): 289–302. https://doi.org/10.1016/j.crte.2007.02.002

Rocca, F., Prati, C. & Ferreti, A. 2014. An overview of SAR interferometry. ESA earthnet online. http://earth.esa.int/workshops/ers97/program-details/speeches/rocca-et-al/ (consulted in April 2018).

Rosen, P.A., Zebker, H., Gurrola, E., Sacco, G., Simmons, M., Hensley, S. & Sandwell, D. 2009. InSAR scientific computing environment. AGU Fall Meeting 2009. Abstract id. IN13C–02. San Francisco, USA.

Rosen, P.A., Gurrola, E., Sacco, G.F. & Zebker, H. 2012. The InSAR scientific computing environment. 9th European Conference on Synthetic Aperture Radar. EUSAR, Memoirs, p. 730–733. Nuremberg, Germany.

Rosen, P.A., Gurrola, E.M., Agram, P.S., Sacco, G.F. & Lavalle, M. 2015. The InSAR scientific computing environment (ISCE): A python framework for earth science. AGU Fall Meeting 2015. Abstract id. IN11C–1789. San Francisco, USA.

Rudenko, S., Schön, N., Uhlemann, M. & Gendt, G. 2013. Reprocessed height time series for GPS stations. Solid Earth, 4(1): 23–41. https://doi.org/10.5194/se-4-23-2013

Sousa, J.J., Magalhães, L.G., Ruiz, A.M., Sousa, A.M.R. & Cardoso, G. 2013. The viStaMPS tool for visualization and manipulation of time series interferometric results. Computers & Geosciences, 52: 409–421. https://doi.org/10.1016/j.cageo.2012.11.012

Strozzi, T. & Wegmuller, U. 1999. Land subsidence in Mexico City mapped by ERS differential SAR interferometry. IEEE International Geoscience and Remote Sensing Symposium. Proceedings, 4, p. 1940–1942. Hamburg, Germany. https://doi.org/10.1109/IGARSS.1999.774993

Teatini, P., Strozzi, T., Tosi, L., Wegmuller, U., Werner, C. & Carbognin, L. 2007. Assessing short–and long–time displacements in the Venice coastland by synthetic aperture radar interferometric point target analysis. Journal of Geophys-

Mapping Land Subsidence in Bogotá, Colombia, Using the Interferometric Synthetic Aperture Radar (InSAR) Technique with TerraSAR–X Images

Quaternary

ical Research: Earth Surface, 112(F1): 1–17. https://doi.org/10.1029/2006JF000656

Tesauro, M., Berardino, P., Lanari, R., Sansosti, E., Fornaro, G. & Franceschetti, G. 2000. Urban subsidence inside the city of Napoli (Italy) observed by satellite radar interferometry. Geophysical Research Letters, 27(13): 1961–1964. https://doi.org/10.1029/2000GL008481

Tomás, R., Herrera, G., Delgado, J. & Peña, F. 2009. Subsidencia del terreno. Enseñanza de las Ciencias de la Tierra, 17(3): 295–302.

UNESCO. 2018. The UNESCO Working Group on Land Subsidence. http://landsubsidence-unesco.org/ (consulted in April 9, 2018)

Universidad Nacional Autónoma de México. 2017. Subsidencia urbana. http://cardi.geofisica.unam.mx/subsidencia/index.html (consulted in December 2017).

Universidad Nacional de Colombia. 2011. Estudio de modelación geotécnica del fenómeno de subsidencia en la ciudad de Bogotá. Contrato 415 de 2010 FOPAE. Final report 1, 175 p. Bogotá.

U.S. Geological Survey. 2017. Measuring land subsidence, InSAR. https://ca.water.usgs.gov/land_subsidence/california-subsidence-measuring.html (consulted in April 2018).

van der Hammen, T., Werner, J.H. & van Dommelen, V. 1973. Palynological record of the upheaval of the northern Andes: A study of the Pliocene and lower Quaternary of the Colombian Eastern Cordillera and the early evolution of its high–Andean biota. Review of Palaeobotany and Palynology, 16(1–2): 1–122. https://doi.org/10.1016/0034-6667(73)90031-6

Veloza, J. 2013. Sistema de modelamiento hidrogeológico del Distrito Capital Bogotá. Secretaría Distrital de Ambiente. Unpublished report, 234 p. Bogotá.

Wegmüller, U., Santoro, M., Werner, C., Strozzi, T., Wiesmann, A. & Lengert, W. 2009. DEM generation using ERS–ENVISAT interferometry. Journal of Applied Geophysics, 69(1): 51–58. https://doi.org/10.1016/j.jappgeo.2009.04.002

Wijninga, V.M. 1996a. Paleobotany and palynology of Neogene sediments from the High Plain of Bogota (Colombia). Evolution of the Andean flora from a paleoecological perspective. Doctoral thesis, University of Amsterdam, 370 p. Amsterdam, the Netherlands.

Wijninga, V.M. 1996b. Neogene ecology of the Salto de Tequendama site (2475 m altitude, cordillera Oriental, Colombia): The paleobotanical record of montane and lowland forests. Review of Palaeobotany and Palynology, 92(1–2): 97–156. https://doi.org/10.1016/0034-6667(94)00100-6

Yuill, B., Lavoie, D. & Reed, D.J. 2009. Understanding subsidence processes in coastal Louisiana. Journal of Coastal Research, SI(54): 23–36. https://doi.org/10.2112/SI54-012.1

Zhou, X., Chang, N.B. & Li, S. 2009. Applications of SAR interferometry in Earth and environmental science research. Sensors, 9(3): 1876–1912. https://doi.org/10.3390/s90301876

Zumberge, J.F., Heflin, M.B., Jefferson, D.C., Watkins, M.M. & Webb, F.H. 1997. Precise point positioning for the efficient and robust analysis of GPS data from large networks. Journal of Geophysical Research: Solid Earth, 102(B3): 5005–5017. https://doi.org/10.1029/96JB03860

Explanation of Acronyms, Abbreviations, and Symbols:

AIST	Advanced Information Systems Technology
ALOS–1, ALOS–2	Advanced Land Observing Satellite
CIC	Cartographic Institute of Catalunya
cGPS	Continuous Global Positioning System
Cosmo–SkyMed	Constellation of Small Satellites for Mediterranean basin Observatory
DAMA	Departamento Administrativo del Medio Ambiente
DEM	Digital elevation model
DLR	Deutsches Zentrum für Luft– und Raumfahrt (German Aerospace Center)
Envisat	ENVIronmental SATellite
ERS–1, ERS–2	European Remote Sensing Satellite
ESTO	Earth Science Technology Office
FHI	Formal Housing Index
FOPAE	Fondo para la Prevención y Atención de Emergencias
GeoRED	Geodesia: Red de Estudios de Deformación
GIAnT	Generic InSAR Analysis Toolbox
GNSS	Global Navigation Satellite System
GPS	Global Positioning System
IGAC	Instituto Geográfico Agustín Codazzi
InSAR	Interferometric synthetic aperture radar
ISCE	InSAR Scientific Computing Environment
JPL	Jet Propulsion Laboratory
LOS	Line–of–sight
MLE	Maximum likelihood estimation
NASA	National Aeronautics and Space Administration
NISAR	NASA–ISRO SAR (NASA– Indian Space Research Organization synthetic aperture radar)
NSBAS	New Small Baseline Subset
RADARSAT–1, RADARSAT–2	Canada´s Earth observation satellite
SAR	Synthetic Aperture Radar
SBAS	Small baseline subset

SEGAL	Space & Earth Geodetic Analysis Laboratory at the University of Beira Interior	TerraSAR–X	German Earth–observation satellite
SGC	Servicio Geológico Colombiano	TDR	Time domain reflectometry
SRTM	Shuttle Radar Topography Mission	UNESCO	United Nations Educational Scientific and Cultural Organization

---

Authors' Biographical Notes

Héctor MORA–PÁEZ has been linked for more than 30 years to tectonic and volcano geodesy research projects to study the deformation of the Earth's crust. He graduated as cadastral and geodetic engineer from the Universidad Distrital of Bogotá, Colombia, obtained a MS from the University of South Carolina, USA, and a PhD from the University of Nagoya, Japan. He is currently the coordinator of the Space Geodesy Research Group at the Servicio Geológico Colombiano, under which the project named Implementation of the GNSS National Network of permanent stations for geodynamic purposes–GeoRED is carried out, a proposal that he presented in 2006. He started working in tectonic geodesy in the CASA project, gathering data in the field, coordinating field campaigns, and processing data from stations located in Costa Rica, Panamá, Colombia, Venezuela, and Ecuador. At the end of the CASA project, he led a construction plan for GPS field stations and data collection, with loan of geodetic equipment from UNAVCO.

Fredy DÍAZ–MILA is member of the Space Geodesy Research Group (GIGE) of the Servicio Geológico Colombiano. His current research is on the application of imaging geodesy techniques for determining movements of the Earth's crust related to geodynamic phenomena, especially interferometric synthetic aperture radar (InSAR). He graduated as a cadastral and geodetic engineer from the Universidad Distrital Francisco José de Caldas and later specialized in geographic information systems at the Universidad Antonio Nariño in Bogotá, Colombia. He obtained a master's in environmental management from the Universidad Internacional Iberoamericana de Puerto Rico. He has coauthored several publications on the use of spatial geodetic technology to analyze the Earth's deformation under the auspices of GIGE.

Leonardo CARDONA is a cadastral and geodetic engineer, and a specialist in spatial analysis at the Universidad Nacional de Colombia. He is a master's candidate in information and communication sciences with specialization in geomatics at Universidad Distrital Francisco José de Caldas. He worked in the Space Geodesy Research Group (GIGE) of the Servicio Geológico Colombiano between 2014 and 2018, supporting the management, processing, and analysis of spatial geodetic information collected from the National Network of GPS Geodetic Stations for geodynamics analysis. He is currently a consultant and also conducts research on the use of spatial geodetic data and information integration.